NASA Technical Memorandum 85748

CONCEPTS FOR IMPROVING THE DAMAGE TOLERANCE OF COMPOSITE COMPRESSION PANELS

Marvin D. Rhodes
Jerry G. Williams

February 1984

NΛSΛ

CONCEPTS FOR IMPROVING THE DAMAGE TOLERANCE

OF COMPOSITE COMPRESSION PANELS

By

Marvin D. Rhodes and Jerry G. Williams

INTRODUCTION

Visual inspection and fail-safe design are key elements in insuring structural integrity of commercial transport aircraft. The current state-of-the-art for fail-safe design of tension-loaded metallic structures has been developed through years of experience. Some design concepts which have proved effective in metallic structures may carry over to the design of tension-loaded composite structures. Flaws and defects in compression-loaded metallic structures are generally of no concern because compression loading does not cause defects to propagate. On the other hand, in compression-loaded composite structures, flaws and defects can be a major concern. Recent tests (refs. 1 – 3) on compression-loaded graphite-epoxy composite structures indicate that local impact-induced damage may propagate by either progressive delamination or local shear instability causing significant strength reductions. This damage may occur during routine aircraft service and maintenance, unavoidable encounters with hailstones, or from an engine rotor burst. Even damage that is not visually detectable may cause appreciable degradation in compression strength (ref. 3). This fact is of special concern because imposing inspection criteria more severe than the visual procedures currently employed may be unacceptable to the airlines and may severely restrict the use of composites by the aircraft manufacturers. Although composites have been introduced into commercial service in secondary structural components (ref. 4), these components operate at design ultimate strains sufficiently low that impact damage does not degrade their structural performance. Heavily-loaded primary structures such as wing panels, however, are designed to efficiently carry loads at high strains and structural performance may be degraded by impact damage.

The current investigation was conducted to evaluate experimentally (1) concepts for improving the compression strength of graphite-epoxy structural panels when subjected to low-velocity impact damage, and (2) concepts for arresting or limiting the growth of damage propagation. Preliminary results of this investigation are presented and discussed in the present paper. Tests were conducted on moderately thick laminated plates (most were about 0.7 cm thick) and on stiffened compression panels representative of structures which have application in heavily-loaded commercial aircraft wings. These tests consisted of impacting specimens while under inplane-axial-compression load. Specimens that did not fail at impact were tested to determine the residual strength. In addition, a structural efficiency analysis was performed to examine the mass penalty imposed by incorporating some of the damage tolerant-features in stiffened compression panel design. The implication of the test results on the design of aircraft structures was examined with regard to FAR requirements.

MATERIALS AND SPECIMENS

Materials

The graphite used in this investigation was a commercially available, high-strength, continuous filament material. The fiber (Thornel 300[1]) was used in both unidirectional tape and bidirectional balanced-weave fabric forms. The tape and fabric were purchased from vendors in a preimpregnated form and kept under refrigeration in sealed containers until ready for use. Three 450K cure thermosetting epoxy-resin prepreg systems were evaluated. Each system was procured from a different supplier and processed in an autoclave according to the manufacturer's recommended procedure. Representative properties of these systems, obtained during the investigation reported in reference 5, are given in table I. The system designated Material A (Rigidite 5208[2]) is a widely used commercially available, high-flow resin system and was chosen because it is representative of systems used in many secondary flight components. Material B (Cycom 907[3]) is a commercially available, low-flow system that has been used in helicopter applications and, to a limited extent, in secondary flight components. Material C is an experimental system formulated by the Ciba Geigy Corporation specifically to improve damage-tolerant characteristics and is not commercially available.

Specimens

Two types of test specimens, flat plates and blade stiffened panels, were evaluated in this investigation. Both types of specimens are representative of structures that may be incorporated in heavily-loaded sections of aircraft wings. All specimens were fabricated using conventional fabrication procedures and autoclave cured. They were cut to size using diamond-impregnated tooling, and the ends to be loaded were ground flat and parallel. Most specimens were inspected ultrasonically to assure freedom from disbonds and foreign inclusions, and one side was painted white to reflect light so a moire-fringe technique could be used to monitor out-of-plane deformations.

Plate specimens. - The plate specimens tested are indicated in table 2 and a sketch is shown in figure 1. The specimen groups (P1 - P5) shown in figure 1(a) were used to study the effect of matrix and graphite material-form on the compression strength of graphite-epoxy laminates with impact damage. The laminated plates with transverse reinforcement, using fibers sewn through the

---

thickness of the plate, (table 2) were fabricated to evaluate the potential of transverse-fiber reinforcement in reducing impact damage. An unreinforced counterpart of each type is included in the tests of laminated plate groups (P1, P2 and P4). The reinforced specimens were stitched with an aramid thread material using a 0.64 cm square grid in the impact region near the specimen center. The stitching was performed prior to autoclave cure.

The discrete-stiffness specimens shown in figure 1(b) were fabricated to evaluate the concept of lumping or isolating a plate into regions of high and low axial stiffness as a means of arresting damage propagation. Regions of low axial stiffness (only $\pm 45^\circ$ plies) have been shown by tests reported in reference 1 to be tolerant to impact. The discrete-stiffness specimens were designed to have the same amount of 0°, 45° and 90° material in the plate as contained in an equivalent width plate of the P2 orientation. The width of the high- and low-stiffness regions was arbitrarily selected.

Another technique investigated for arresting propagating damage was the mechanically fastening of sections of plates together (table 2) using high-strength steel bolts (figure 1(c)). Several specimens were assembled and tested using the P1 laminated plates fastened together with 0.95 cm diameter aircraft bolts. The bolt size and spacing were arbitrarily selected.

Blade-stiffened panels. - Two types of blade-stiffened panels were evaluated. The first type consisted of traditional blade sections attached to, or cocured with, a continuous skin. The second type consisted of a series of channel sections bolted together along the flange.

The first type was designed using a computerized-sizing-program, PASCO (Panel Analysis and Sizing Code), and is illustrated in figure 2. A discussion of PASCO capabilities are given in reference 6 and examples of its application may be found in reference 7. Configuration details and dimensions of the test panels are summarized in table 3. The panels were designed to have a minimum mass W/AL (panel mass per unit surface area per unit length) subject to an in-plane axial compression loading and a number of practical constraints. The axial compression load requirements were between 2.63 - 3.33 MN/m, which is representative of heavily-loaded upper-surface aluminum wing panels on current commercial aircraft. The constraints considered in the design process included buckling, in-plane and shear stiffnesses equal to or greater than aluminum wing panels of the same load capability, bow-type imperfections along the panel length, practical dimensions and material strength limitations. The effect some of these constraints have on panel mass are discussed in reference 7.

Several damage-tolerant features investigated in the plate specimens were incorporated in the first type of blade-stiffened panels. Panels with bonded or mechanically attached stiffeners were compared with those having cocurred stiffeners. Several of the panels with bonded or mechanically attached stiffeners also incorporated discrete-stiffening concepts similar to the plate specimens. The skin of these stiffened panels was primarily $\pm 45^\circ$ material to give a low-modulus section and the stiffeners were primarily 0° material to give a high modulus in the blade and flange. The two commercially available materials, Material A and Material B, were used to fabricate test panels.

The panel mass parameter, obtained from PASCO, is shown in figure 3 as a function of the load index for blade-stiffened graphite-epoxy panels. These panels were required to carry the specified compression load subject to the following conditions: (a) have extensional and shear stiffnesses representative of commercial aircraft wing panels (ref. 7), (b) to be resistant to buckling, (c) to have a maximum average strain of 0.005 or less, (d) to have a bow-type imperfection along a 76 cm length of 0.23 cm, and (e) to have a maximum strain including the effect of the bow of less than 0.0067. The bonded region in figure 3 represents the mass and loading for typical commercial aircraft aluminum wing panels. The test panels represent considerable mass savings when compared to the aluminum wing panels. Deviations from the minimum-mass curve for the test panels are a consequence of changes to optimum designs made to reduce the allowable strain and to simplify manufacturing.

The second type of blade-stiffened panel involving a series of channel sections mechanically fastened together is shown in figure 4. This concept is of interest for two reasons. First, mechanical fastening was evaluated as a damage-arrestment technique; and second, panels of this type could be assembled from pultruded sections thus potentially reducing fabrication costs. Two panels were fabricated from Material A using the same fiber orientation as the P1 plate specimen group (table 2). The channels were of uniform cross-section; therefore, the blades of the test panels were twice as thick as the skin. These panels were fabricated for a conceptual study only, and the P1 plate laminate was selected because the impact characteristics were well defined from tests on plate specimens. The concept may be easily evaluated by comparing test results with those of the plate specimens. Panels sized using the PASCO program could be studied for further evaluation of efficient structural designs. The sections of the test panels were fastened together using 0.95 cm diameter high-strength aircraft bolts. The spacing of the fasteners and the dimensional configuration of the specimens were arbitrarily selected.

APPARATUS AND TESTS

Apparatus

The plate test specimens, with nominal dimensions of 12 x 25 cm, were supported in a frame similar to the one shown in figure 5. The frame consists of two adjustable side supports and adjustable end supports at the top and bottom. The side supports simulate simple-support boundary conditions and were placed approximately 0.6 cm from the specimen edge. The end supports simulate a clamped boundary condition. The wider plate specimens were supported in a similar test frame that included two additional interior simple supports along a line on each side of the specimen. They were located at one-third the specimen width from the edge to prevent buckling. No special apparatus or side supports were required for the blade-stiffened panels.

A conventional hydraulic loading machine was used to load the plate and panel specimens in compression. Electrical resistance strain gages were bonded to the specimen to monitor the applied axial strain and bending strains caused by out-of-plane deformations. The gages were placed at locations away from the impact region and bolts, where local effects would not influence the

measured values. Displacements of the loading platens and out-of-plane deformations normal to the panel surface were monitored by direct-current differential transformers. Electrical signals from all strain gages, displacement transducers and the load transducer were recorded on magnetic tape at regular time intervals during the test.

Solid aluminum spheres 1.27 cm in diameter with a mass of 3 grams were used as the impact projectiles for studies on both the flat plates and stiffened panels. The spheres were propelled by a compressed air gun which had an electronic detector mounted on the end of the barrel to measure projectile speed. Additional information on the air gun and its operation can be found in reference 1.

Ultrasonic C-scan flaw detection equipment was used to evaluate the extent and location of the region damaged by impact. The equipment consisted of a focused high-resolution pulse-echo type piezoelectric transducer, a tank for immersion of the transducer and specimen in a water bath, and a transversing mechanism to scan automatically the specimen surface.

Tests

Undamaged control specimens were loaded in compression to determine the critical load and strain at buckling and the applied load at failure. Buckling was defined by the load-strain response and strain-reversal technique. The strain measurements were complemented by the moire-fringe method for observing contours of out-of-plane deformation which provided visual definition of the buckled mode-shape.

Test specimens were damaged by impact near the center while under static compression load to evaluate the effect of discrete-source damage. Some of these specimens continued to carry load while others failed. Those panels that continued to carry load were inspected visually and some were examined ultrasonically. Most were then loaded in compression to failure to determine their residual strength. The remaining specimens with damage were sectioned using a diamond-impregnated saw, and the cross-sections were examined using microscopes. This inspection technique was used to evaluate details of the interior laminate damage.

RESULTS AND DISCUSSION

Plate Specimens

Matrix materials. - The effect of impact damage on the compression strength of the orthotropic plate specimen groups, P1 - P3, is shown in figure 6. The ordinates in figure 6 are axial strains measured on the specimen due to the applied compression load, and the abscissas are projectile impact velocities. The solid circular symbols (fig. 6a - 6c) represent specimens that failed due to projectile impact while the open circles represent specimens that did not fail even though they may have incurred some local damage. A curve labeled "failure threshold" has been faired between the open and solid circular symbols of each

set of data shown to represent a lower bound to the applied static compression strain that causes failure at a given velocity for the impact projectile used. Data points on the ordinate are failures of undamaged control specimens. These specimens failed after buckling and, therefore, do not represent the ultimate static strength of the test laminates. The specimens that did not fail due to impact, as well as several that were damaged without an applied static load, were subsequently tested to determine their residual compression strength. These results are shown by the solid square symbols on figure 6. Every data point representing the residual compression strength is on or above the failure-threshold curve. This suggests that impacting test specimens while under load is an effective method of establishing a lower bound for the residual static compression strain of graphite-epoxy laminates damaged by low-velocity impact. Specimens damaged by impact at 50 to 75 m/s failed during residual strength tests at about the same strain as the undamaged control specimens even though the failure may have occurred through the impact location.

Also shown on figure 6 is the impact velocity at which surface damage becomes visually detectable on both the contact surface and the back surface of the laminate. These data were obtained from specimens that were damaged at approximately eight different impact velocities (without load). The impact regions were carefully inspected by several individuals, some with previous aircraft technician service experience. The velocity range for these tests exceeded that used to determine the failure-threshold curve. The wide bands shown in figure 6 denote uncertainty involved in detecting visual damage. The first evidence of damage in the contact region is a very shallow circular depression which is difficult to see. The first evidence of damage on the rear surface is a small crack in the surface ply. As impact velocity increases, the front surface circular depression becomes more pronounced, and portions of the rear surface ply may delaminate or spall off. It is apparent from the data that severe reductions in compression strength may occur from damage that is marginally detectable by unaided visual inspection. Materials B and C, with the higher damage-tolerant capability, also require higher velocity to impose visually detectable damage. Design implications of this finding are discussed in a subsequent section.

A comparison of the failure-threshold curves shown in figure 6d demonstrates clearly that the matrix material has considerable effect on impact damage tolerance since the same graphite fiber was used with each material evaluated. It is believed that this result may be related to differences in the failure mode. Two modes of failure in compression loaded composite laminates; delamination and transverse-shear crippling, have been identified and are discussed in references 3 and 8. Delamination due to impact generally occurs at ply interfaces where there is a major change in the angle between plies, e.g., between $0°$ and $45°$ plies. The sublaminates formed by delamination have a low bending stiffness and may buckle locally at a load well below the buckling load of the undamaged panel. The local buckling creates high transverse tension and peel stresses at the delamination boundary which cause the damage to propagate. If the propagation is not arrested or the load is not redistributed, the damage propagates until the panel fails by general instability. The transverse-shear failure mode is caused by a shear instability in the high-axial-stiffness $0°$ plies (see additional discussion in reference 9) in which the length of the crippled fibers may be only 4 or 5 fiber diameters. A specimen that has failed by transverse shear usually exhibits delamination

in the cross section due to wedging of the failed plies at the interfaces. Failures by both modes propagate laterally across the width of the specimen. Damaged panels fabricated from Material A usually fail at low compression loads by delamination while those fabricated from Materials B and C fail primarily by transverse-shear crippling.

Graphite fabric. - The results of impact tests on predominately graphite fabric laminates (plate groups P4 and P5, table 2) are shown in figure 7. These results are compared with the failure-threshold curves for all-tape laminates with similar orthotropic properties presented in figure 6 and reference 3. The failure-threshold curves for the fabric specimens at velocities greater than 100 m/s are 25 - 30 percent higher than for the all-tape laminates. The specific reason for the improvement is unclear, however, it has been noted that impact initiated failures are most pronounced where there is a major change in ply angle. The cross-plies of woven graphite material are mechanically linked together, thereby reducing the number of interfaces available to participate in delamination. The regions of visually detectable damage for the fabric laminates are also shown on figure 7. The damage on the back surface of these specimens is notably easier to detect than it is in the contact region. This is in contrast to the tape laminates shown in figure 6 and the reason for this is unclear. However, the nature of damage (shallow circular depression) makes detection very subjective and can be influenced by surface finish and lighting.

Transverse reinforcement. - The results of tests on plate groups RP1 - RP3 conducted to evaluate the effect of stitching are shown in figure 8. Also shown on the figure is the failure-threshold curve for plates without stitching fabricated from the same matrix systems. The transverse reinforcement significantly increases the failure threshold of those plates fabricated from Material A (RP1 and RP3), however, there is little or no difference in the failure-threshold curves for plates fabricated from Material B. Note that the residual strength of reinforced plates fabricated from Material A tape (RP1) is somewhat higher than the failure-threshold curve, and that a curve faired through the residual strength data would be about the same as the threshold curve for Material B. This is believed due to the plate failure modes. As indicated previously, the unreinforced plates of the Material A tape fail primarily by delamination. Transverse reinforcement in plates of this material is adequate to suppress delamination and mechanically locks the laminate together, thereby restricting the failure to a higher-energy transverse-shear mode. Additional reinforcement of Material B, however, is unnecessary and plates with and without reinforcement fail by transverse shear, a mode related to the shear modulus of the matrix materials (ref. 9). Although additional tests will be required to evaluate these effects, the Material B failure-threshold curve may represent an intrinsic material property of this class of graphite-epoxy materials with impact damage and improvements may require an increase in the matrix shear modulus.

Transverse reinforcement appears to reduce the extent of interior impact damage as shown in figure 9. This data was obtained by ultrasonic inspection of laminates fabricated from Material A, after impact at different velocities. Both laminates evaluated at the same projectile velocity had smaller regions of damage with transverse reinforcement than those which had no reinforcement. Several stitched specimens were cross-sectioned to examine the nature of the interior laminate damage and photographs of two such cross sections are shown

in figure 10. The interior laminate damage is similar to that observed in unreinforced specimens reported in reference 3. The reinforcement, however, does appear to restrict slightly the extent of interlaminar cracking which is why the damage area, as determined by C-scan inspection (fig. 9), was somewhat smaller. It should also be noted in figure 10 that the specimens had voids in the vicinity of the reinforcing thread which are near or below the level of C-scan detection. These voids did not reduce the strength of the control specimens which failed after buckling and apparently had no deleterious effect on specimens damaged by impact.

Discrete-stiffness design. - The plates constructed from the Material B with regions of discrete stiffness were proof tested to a strain in excess of 0.0060. They were then damaged by impact in the low-axial-stiffness region to further substantiate test results reported in reference 1 which indicated these regions should be damage tolerant. The first test plate was damaged by impact without load and the second was damaged while loaded to a strain of about 0.0053. Both had easily detectable visible damage and were subsequently proof loaded to a strain of 0.0060. No propagation or increase in the size of the damage occurred. The results of impact in the high-axial-stiffness region are shown in figure 11. One plate as indicated by the open symbol was damaged while loaded to an applied strain of 0.0044. No propagation of damage occurred and the specimen was subsequently loaded to a strain of about 0.0055 at which the damage propagated across the center high-stiffness region and arrested. The propagation was apparently by shear crippling in the 0° plies and there was no apparent propagation into the low-axial-stiffness, $\pm45^\circ$, region. The second test plate was damaged while loaded at an applied axial strain of about 0.0054. Upon impact, the high-axial-stiffness region failed similar to the damage propagation of the first panel. The results of tests on both test specimens demonstrate the effectiveness of discrete stiffness in containing propagating damage.

Mechanically fastened plates. - Results of tests on two plates fabricated using mechanical fasteners (table 2) are shown in figure 12. Also shown in the figure is the failure-threshold curve from figure 6a for the orthotropic plates of Material A. The applied strain at impact is indicated by the open circle. Both test specimens were damaged while under load at an applied strain sufficiently high to ensure that the damage would propagate. The damage initiated failure of the center plate but did not propagate into either side plate. The strain recorded in the side plates after failure of the center section is indicated by the partially filled circle. These tests demonstrate experimentally that mechanical fastening may be an effective technique for confining propagating damage to a controlled region.

Blade-Stiffened Panels

The configuration details incorporated in the blade-stiffened panels are given in table 3 and the results of proof, impact, and residual strength tests on these panels are summarized in table 4. The skin elements in the panels ranged in thickness from 22 to 42 plies and all impacts were in the panel skin. Based on the plate specimen results previously discussed, the impact conditions selected for these tests (table 4) were intended to be moderately severe.

Panels 1a, 1b and 2 were fabricated and tested to evaluate the concept of attached or bonded-on-stiffeners versus cocured-integral-blade stiffeners. Both designs had the same configuration dimensions and ply orientations based on a minimum-mass integrally stiffened design developed using the PASCO program. The stiffeners of panel 2 were modified slightly to provide a 7.6 cm wide flange, 12 plies thick for bonding the stiffener to the panel skin. Two test panels of configuration 1 and one panel of configuration 2 were tested under similar impact conditions. All of the panels failed due to impact induced skin-delamination which propagated completely across the panel permitting the sublaminates in the skin to buckle locally. A photograph of a typical skin-stiffener intersection cut from panel 1 after failure is shown in Figure 13. It is apparent from an examination of this cross-section that there are multiple planes of delamination and the delaminations have propagated in about the same plane. Also, the delamination did not propagate into the stiffener thereby permitting the panel to have significant residual strength following the delamination failure. The reason the delaminations did not propagate into the stiffener is that the high-stiffness, 0°, plies do not traverse into the stiffener thereby denying the delamination a natural path into the stiffener. The skin attached to the stiffeners was adequate to stabilize the stiffeners in these short panels. In longer panels lateral or rolling stability of the stiffener could become significant at lower loads in residual-strength tests. Since 0° skin plies for both designs 1 and 2 do not traverse into the stiffener, and due to the characteristic skin delamination failure mode, the bonded stiffener concept provided no improvement in damage tolerance compared to the cocured design.

Test panels 3 and 4 were designed to provide the principal axial stiffness in the blade stiffeners and the required shear stiffness in the panel skin. The skin was composed predominantly of $\pm 45^\circ$ plies and included no high-axial-stiffness, 0°, plies. (This configuration is similar to the discrete-stiffness plates discussed previously). A $\pm 45^\circ$ laminate, however, has a high Poisson's ratio ($\sim .71$) and several 90° plies were included in the skin to reduce the lateral expansion. Even with these 90° plies, Poisson's ratio is still high ($\sim .53$). This design resulted in a moderately wide stiffener spacing of 22.4 cm as noted in the dimensions for panel 3 included in table 3. During the initial control test on panel 3, the skin buckled at an applied axial strain of .003. This was due to combined loads introduced in the skin. These loads were the applied axial load and a lateral load resulting from restraining the Poisson's expansion of the skin. This restraint is imposed by frictional forces between the panel ends and the test machine platens. The high lateral bending stiffness of the stiffeners do not permit the skin to expand laterally. Panel 3 was damaged by impact with the skin in a buckled condition and some test results are illustrated in figure 14. Following impact, the panel was evaluated by C-scan inspection and the photograph shown in figure 14a indicates there was moderate local damage. The dark regions along the edge of the stiffener flange are due to variations in bond-line thickness and are unrelated to the impact damage. Subsequent loading of panel 3 to an applied strain of 0.0042 caused the damage to propagate laterally across the skin and arrest beneath the stiffener flange as noted by the C-scan photograph, figure 14b. The damage propagation was also evident in the load-strain response curves of figure 14c. In a subsequent test on this panel, a load of 3.77 MN/m caused no further damage propagation even though there was considerable post-buckling deformation in the panel skin (figure 14d).

Test panel 4 was similar in design and laminate configuration to panel 3 except the skin was attached to the stiffeners by titanium flush-head inter- ference-fit bolts and the stiffener spacing was reduced to 15.2 cm to increase the buckling strain of the skin. Tests results noted in table 4 indicate panel 4 was tolerant to impact damage in the skin under high loading conditions and the residual strength with damage was also high. The discrete-stiffness con- cept incorporated in both panels 3 and 4 was very tolerant to damage in the panel skin, even with considerable post-buckling. Further tests on this concept, however, should be conducted to evaluate the effectiveness of the skin in re- distributing load in the event of stiffener failure.

Test panels 6 and 7 have similar stiffener dimensions and were used to evaluate the effect of material on damage tolerance. Panel 6 was fabricated using Material A and panel 7 was fabricated from Material B. Due to differences in lamina elastic properties of the two materials, the two panels have slightly different layup patterns and are capable of carrying different design loads. The test results given in table 4 show that panel 6 performed in a manner similar to panel 3. Following impact, the local damage propagated in the skin to the adjacent stiffeners where it arrested. The local damage to the skin of panel 7 did not propagate and the panel failed in the residual-strength test at a strain of 0.0060 by disbonding of the stiffeners from the skin. There was no evidence of damage growth in the impact region.

Test panel 5 incorporated all three damage-tolerant features previously evaluated separately in other panels (low-axial-stiffness skin, attached stif- feners, and alternate materials). This test panel failed in the end-region at a strain of 0.0054 (table 4) with no evidence of damage growth. Even though the failure occurred at a moderately high strain, it is unclear when comparing the results to those of panel 7 if all three damage tolerance features con- tributed to the success of this test or only the alternate material.

During tests on panels 3 and 6, delamination initiated at the impact location propagated across the skin to the two adjacent stiffeners and arrested as noted in sketch A. It is hypothesized that the feature in these panels
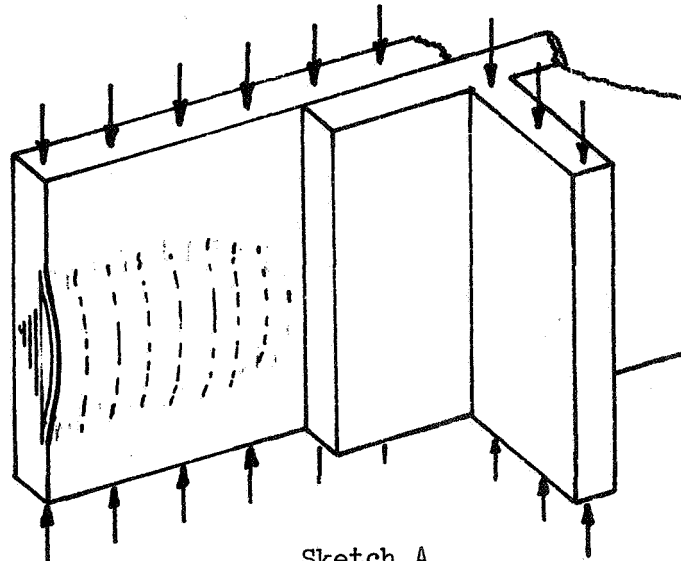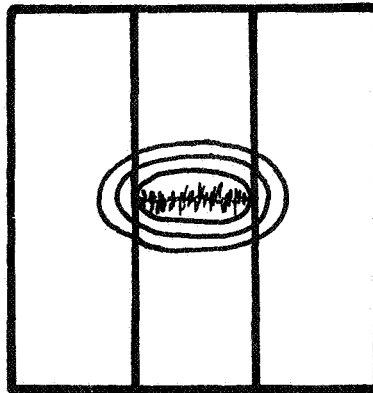

Sketch A

responsible for the delamination arrestment is the relatively thick blade and
attachment flange. The blade and flange had sufficient bending stiffness to
constrain local buckling of the skin sublaminates. Local buckling creates high
peel stresses which are a major factor in delamination growth. The local
buckling restraint imposed by the stiffener, therefore, provides an effective
mechanism for arresting a delamination propagation.

Due to the limited number of panels tested, the merit associated with
combining damage-tolerant features in a single panel design could not be
evaluated. Also, the merit of these concepts must be explored in tests on
longer and wider panels to address the consequence of stiffener failure and the
subsequent effect of load redistribution. It was anticipated that the test on
panel 4 which had the skin secured by bolts might provide insight in load re-
distribution through local bolt bearing failures, however, this panel was too
short to effectively evaluate the concept. The test results demonstrate the
damage-tolerant features incorporated in the blade-stiffened panels have merit
when compared to tests previously conducted and reported in reference 7. The
heavily-loaded blade-stiffened panels reported in reference 7 failed due to
impact when loaded at strains near 0.0040. Several of the panels evaluated in
the current study were able to sustain load under similar impact conditions
and had residual strength with damage at strains well in excess of 0.0050.
The low-axial-stiffness skin, the use of alternate materials and the restraint
of local buckling are all effective methods of suppressing damage propagation.

Results from tests on two channel-section blade-stiffened panels are shown
in figure 15. The applied strain at impact is shown on the figure in a manner
similar to previous figures. These test panels failed in the center section
due to impact and the damage propagated into the blade portion of this section
because the skin plies traverse into the stiffener. However, the damage
arrested at the interface where the sections were fastened together. One panel
was subsequently loaded to establish its ultimate strength. Failure originated
near the center-section damage and propagated to the panel lateral edges. A
moire-fringe grid was used to observe the out-of-plane deformation of the flat
surface during the test. The deformation contours observed indicated that the
panel failed due to eccentricities imposed by load transfer around the failure
in the center section (see sketch B). Load transfer and severe eccentricities

Sketch B

imposed by local failures, particularly at stiffeners, must be accounted for
in the design of stiffened compression panels.

DESIGN IMPLICATION STUDIES

Impact Damage

For conventional metallic structures, fatigue usually governs the design of tension-loaded panels and buckling or material strength requirements govern the design of compression-loaded panels. The design considerations for aluminum aircraft panels have evolved over 30 years and are based on requirements defined by Federal Aviation Regulations (FAR., ref. 10). The regulations state basically that aircraft structures must be capable of supporting limit load, the maximum load to be expected in service. Ultimate load is defined as 1.5 times the limit load. The structure must be capable of supporting limit load without detrimental permanent deformation and must be able to support static-ultimate load for at least three seconds without failure. An evaluation of the strength, detail design, and fabrication must show that catastrophic failure due to fatigue, corrosion, or accidental damage will be avoided throughout the operational life of the airplane. The extent of damage for residual strength evaluation at any time within the operational life must be consistent with initial detectability and subsequent growth under repeated loads. The residual strength evaluation with damage must show that the remaining structure is able to withstand loads corresponding to certain maneuver and gust conditions. In addition, the aircraft must be capable of successfully completing a flight during which damage occurs, with the structure under load, from discrete sources such as uncontained fan blades, uncontained high-energy rotating machinery, or hail stones (ref. 11). Although the regulations were formulated through experience with aluminum structures, they are generally written and apply equally well to tension- or compression-dominated metallic structures, as well as laminated composite structures.

For illustrative purposes, a damage-threshold curve for a composite material with impact properties based on the type of test performed in this investigation is shown in figure 16 along with FAR requirements noted above. In the figure, strains have been shown rather than stresses or loads. The limit and ultimate design strains on the curve are values that are currently used for aluminum wing panels and are reasonable values for consideration in the design of graphite-epoxy wing panels. Damage from discrete sources is not considered to be a major problem in the design of aluminum compression structures, therefore, no information on a design strain level is available. The strain level shown is an anticipated level (neglecting the relation of panel to impactor-size effects) based on encountering wind gusts during an inflight hail storm. This condition is normally less severe than the design limit load. In addition, it would be desirable for the lowest impact condition necessary to create interior laminate damage to also cause surface damage that is visually detectable in the contact region. As indicated, the region of uncertainty with regard to visual-damage detectability should be small.

The materials and laminates tested in this investigation had a residual compression strength with damage that was near or above the failure-threshold curve. Assuming other materials and laminates also exhibit this character, the test technique reported herein can be used to predict the curve for the lower threshold of residual strength. This curve should fall in the region indicated in figure 16. For impact damage which is not visually detectable, it must plot

above the established design ultimate, and for damage which is visually detectable, it must plot above the design limit. For materials that exhibit this behavior, discrete-source damage will not be a problem.

The results of tests on the laminates fabricated from Materials A and B are compared in figure 17(a) and (b) with the design strain considerations defined in figure 16. Both laminates appear capable of meeting the anticipated discrete-source limit, however, the failure-threshold curves are low with regard to the defined region of visible contact damage. If the design-limit strain (and corresponding design ultimate strain) was reduced moderately, Material B may be adequate (assuming it will fulfill all other requirements). Also recall the transverse reinforcement of Material A increased substantially the residual strength of laminates with damage to a level comparable with Material B failure threshold, and reduced the range of uncertainty in visual damage detectability to nearly that of Material B. Consequently, the transverse reinforcement represents a substantial improvement in Material A from the standpoint of its design capability for heavily-loaded wing structures.

An examination of test results on the blade-stiffened panels based on the same design considerations are shown in figure 18. Shown on the figure are the panel strain at impact and the strain at failure of each blade-stiffened panel. Each specimen shown was damaged while loaded to an applied strain well above the limit for discrete-source damage. All panels had surface damage in the contact region that was marginally detectable by visual inspection. This impact damage resulted in failure for panels 1 - 4 and 6 at an applied strain equal to or greater than the indicated design limit value. Test panels 5 and 7 fabricated from the Material B failed due to causes unassociated with impact at strains near the design ultimate for current aluminum panels. These results demonstrate the importance of visual inspection in detecting flaws in composite compression panels.

Structural Efficiency

In addition to safety, one of the main considerations in the design of aircraft is structural mass. The design of blade-stiffened graphite-epoxy panels was discussed in detail in reference 7 and it was demonstrated that composite panels offer substantial mass saving when compared to current aircraft aluminum panels, even when the graphite panels are constrained to meet the same requirements as defined previously for figure 3. The material properties used in the design of the reference 7 panels was that of Material A and damage tolerance was accounted for by simply reducing the design strain level. In the present investigation, other materials with improved damage characteristics have been evaluated. These materials, however, typically have a lower extensional modulus due to higher matrix volume fraction (note the difference in lamina ply thickness of Materials A, B and C given in table 1). Both Materials B and C are "low-bleed" systems and consequently excess resin cannot be easily removed. This reduces the longitudinal modulus 15 to 20 percent when compared to Material A. The effect of reducing the extensional modulus on panel structural mass is shown in figure 19. Also shown on the figure is the mass of typical aircraft aluminum wing panels. The ordinate and abscissa on the figure as well as the constraint conditions considered in the design are similar to those of figure 3.

The effect of reducing the longitudinal modulus of the material from 131 GN/m^2 to 111 GN/m^2 increases the panel mass about 7% when compared to aluminum wing panels throughout the entire load range. For heavily-loaded panels, this has the same effect as reducing the allowable average panel strain for the higher modulus material by 0.0014. However, for lightly-loaded panels, the reduction in allowable strain does not increase panel mass because these panels are stiffness-critical and do not reach the limits of material strength. Tradeoffs such as this should be considered during any design evaluation.

The effect of discrete-stiffness design on structural efficiency was also evaluated and the results for blade-stiffened panels are shown in figure 20. The Material A properties were used to generate these curves and the one representing designs with 0° plies in the skin is the same as the curve shown in figure 19. The curve labeled discrete stiffness has the same constraint conditions as the curve labeled 0° plies in the skin and also satisfies an additional constraint of having only $\pm45^\circ$ and 90° material in the skin. The results of figure 20 show there is a penalty of about 3% for panels with no high-stiffness material in the skin when compared with minimum-mass designs that include 0° plies in the skin. However, a substantial mass saving of between 46 percent for lightly-loaded panels and 37 percent for those designed for about 6 MPa still remains. One important aspect of the discrete-stiffness concept which remains to be evaluated is whether the load can be redistributed in the event of stiffener failure. Long panels (approximately 3 or more rib bays in length) will have to be tested to further evaluate this concept.

<div align="center">CONCLUDING REMARKS</div>

An experimental investigation was conducted to evaluate concepts for improving the strength of graphite-epoxy compression panels subjected to low-velocity impact damage and for arresting damage propagation. Tests were conducted on plate specimens and blade-stiffened structural panels. The plate specimens were 48 ply orthotropic flat laminates. The structural panels were minimum mass to carry the design load and have extensional and shear stiffnesses typical of those found in current commercial aircraft aluminum wing applications. Test results on the plate specimens suggest that the matrix material can have a significant effect on impact-damage tolerance, and matrix materials that fail by delamination have the lowest capability. Alternate materials or laminates which are transversely reinforced suppress delamination and change the failure mode to transverse-shear crippling of the fibers which occurs at a higher strain value. All the laminate groups evaluated had severe reductions in strength that occur from damage that may only be marginally detectable by un-aided visual inspection. Tests on plate specimens that incorporated discrete stiffness or mechanical fasteners to restrain damage propagation demonstrated the effectiveness of these methods to arrest damage propagation and achieve moderately high strains with damage.

The results of tests on the blade-stiffened compression panels indicated several design changes that improve damage tolerance. For materials that fail by delamination, denying the delamination a natural path into the stiffener permits the stiffener to remain intact when the skin is damaged. Also, blades and flanges with bending stiffnesses adequate to constrain local-buckling

deformations provide an effective mechanism for stopping delamination propagation in the panel skin. The techniques of discrete stiffness and the use of alternate materials evaluated in plate specimens were also examined in stiffened panels and found to be effective. Longer panels, however, should be tested to fully evaluate these techniques and to study load redistribution after damage, especially for the case of a failed stiffener.

The implication of the test results on the design of aircraft structures was examined and a composite material with desirable impact characteristics with respect to FAR requirements was defined. The materials evaluated in this investigation appear capable of meeting the requirements for discrete-source damage, however, the failure-threshold curve of the test laminates appears to be low with regard to the initiation of visible contact damage. The effect on structural mass of incorporating the damage-tolerant features in panel designs showed that small penalties exist in using some of the features. However, substantial mass savings compared to existing aluminum panels remain for heavily-loaded structures which include these damage-tolerant concepts.

REFERENCES

1. Rhodes, Marvin D.; Williams, Jerry G.; and Starnes, James H., Jr.: Effect of Impact Damage on the Compression Strength of Filamentary-Composite Hat-Stiffened Panels. Society for the Advancement of Material and Process Engineering, Vol. 23, pp. 300-319, May 1978.

2. Byers, Bruce A.: Behavior of Damaged Graphite/Epoxy Laminates Under Compression Loading. NASA CR 159293, August 1980.

3. Rhodes, Marvin D.; Williams, Jerry G.; and Starnes, James H., Jr.: Low Velocity Impact Damage in Graphite-Fiber Reinforced Epoxy Laminates. Proceedings of 34th Annual Conference Reinforced Plastics/Composite Institute, The Society of the Plastics Industry, Inc., Jan. 29-Feb. 2, 1979.

4. Dexter, H. Benson: Composite Components on Commercial Aircraft. Proceedings of the AGARD Specialist Meeting on Effect of Service Environment on Composite Materials, Athens, Greece, April 13-18, 1980.

5. Palmer, R. J.: Resin Properties to Improve Impact in Composites. Proceedings of the Fifth DOD/NASA Conference on Fibrous Composites in Structural Design, January 27-29, 1981.

6. Anderson, Melvin S.; and Stroud, W. Jefferson: A General Panel Sizing Computer Code and Its Application to Composite Structural Panels. A Collection of Technical Papers - AIAA/ASME 19th Structures, Structural Dynamics and Materials Conference, April 1978, pp. 14-22, AIAA Paper No. 78-467.

7. Williams, Jerry G.; Anderson, Melvin S.; Rhodes, Marvin D.; Starnes, James H., Jr.; and Stroud, W. Jefferson: Recent Developments in the Design, Testing, and Impact-Damage Tolerance of Stiffened Composite Panels. Proceedings of Fourth Conference on Fibrous Composites in Structural Design, San Diego, California, November 14-17, 1978.

8. Rhodes, Marvin D.: Damage Tolerance Research on Composite Compression Panels. Selected NASA Research in Composite Materials and Structures, NASA CP 2142, August 1980.

9. Chaplin, C. R.: Compression Fracture in Unidirectional Glass-Reinforced Plastics. Journal of Material Science, Vol. 12, pp. 347-352, 1977.

10. Anon: Federal Aviation Regulations. Part 25, Airworthiness Standards: Transport Category Airplanes, Subpart C - Structure. Published June 1974.

11. Ferrarese, J. A.: Federal Aviation Administration Advisory Circular. AC #20-107, July 1978.

TABLE I

TYPICAL LONGITUDINAL PROPERTIES OF UNIDIRECTIONAL

GRAPHITE—EPOXY SYSTEMS

Material Property	Material A	Material B	Material C
Compression Strength, GPa	1.45	1.24	1.14
Compression Modulus, GPa	124.1	112.4	---
Short Beam Shear Strength, MPa	131.0	106.9	111.7
Fiber Volume Fraction	0.71	0.68	---
Neat Resin Elongation to Failure	0.010	0.048	0.046
Ply Thickness of Test Panels, mm	0.14	0.15	0.16

TABLE II.- DIMENSIONS AND LAYUP PATTERNS OF FLAT PLATE TEST SPECIMENS
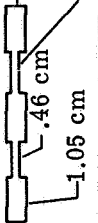
Type	Specimen group	Number of test specimens	Material	Fiber form	Size, cm	Thickness, cm	Lamina orientation
Laminated plate	P1	23	A	Tape	11.4×24.8	0.67	$(\pm45/0_2/\pm45/0_2/\pm45/0/90)_{2s}$
	P2	10	B	Tape	11.4×24.8	0.80	$(\pm45/0_2/\pm45/0_2/\pm45/0/90)_{2s}$
	P3	12	C	Tape	12.7×24.8	0.80	$(\pm45/0_2/\pm45/0_2/\pm45/0/90)_{2s}$
	P4	17	A	Tape/fabric	12.7×25.4	0.79	$(45_f/(0_t)_2/45_f/(0_t)_2/45_f/(0_f)_{2s}$
	P5	14	A	Fabric	12.7×25.4	0.71	$(45/0)_{5s}$
Laminated plate with transverse reinforcement	RP1	11	A	Tape	12.7×25.4	0.68	$(\pm45/0_2/\pm45/0_2/\pm45/0/90)_{2s}$
	RP2	10	B	Tape	12.7×25.4	0.71	$(\pm45/0_2/\pm45/0_2/\pm45/0/90)_{2s}$
	RP3	7	A	Tape/fabric	12.7×25.4	0.78	$(45_f/(0_t)_2/45_f/(0_t)_2/45_f/(0_f)_{2s}$
Discrete stiffness		2	B	Tape	25.4×38.1	.46 cm / 1.05 cm	$(0_5/\pm45/0_5/\pm45/0_5/(\pm45)_3/90/(\pm45)_3/90)_s$ $(\pm(45)_3/90)_{2s}$
Mechanical fastening		3	A	Tape	25.4×29.2		$(\pm45/0_2/\pm45/0_2/\pm45/0/90)_{2s}$

TABLE III.- DIMENSIONS AND LAYUP PATTERNS OF BLADE-STIFFENED TEST SPECIMENS
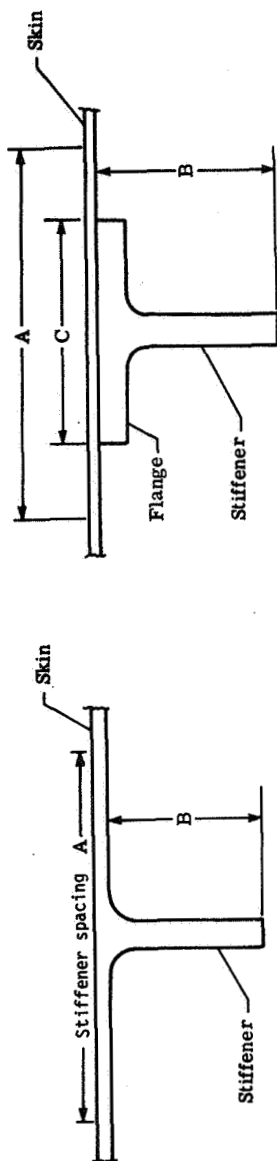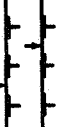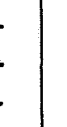
I. Cocurred

II. Attached stiffener

Panel	Design	Material	Design Conditions			Dimensions			Element	Plies	t, cm	Layup Pattern (Orientation)	Damage-tolerant design features
			N_x MN/m	Axial strain	W/A kg/m²	A, cm	B, cm	C, cm					
1	Cocurred	A	2.63	0.0036	15.28	12.7	5.28	---	Skin	42	0.554	$[(\pm45)_6/0_2/90/\pm45/0_2/90/\pm\overline{45}]_s$	0° skin plies do not traverse up into stiffener
									Stiffener	75	0.991	$[\pm45/0_3/90/0_3/\pm45/0_6/\pm45/0_3/90/0_3/\pm45/0_7/\pm\overline{45}]_s$	
2	Bonded	A	2.63	0.0036	16.55	12.7	5.28	7.62	Skin	42	0.554	$[(\pm45)_6/0_2/90/\pm45/0_2/90/\pm\overline{45}]_s$	Discrete stiffener
									Stiffener	75	0.991	$[\pm45/0_3/90/0_3/\pm45/0_6/\pm45/0_3/90/0_3/\pm45/0_7/\pm\overline{45}]_s$	
									Flange	12	0.157	$[\pm45/\pm45/\pm\overline{45}]_s$	
3	Bonded	A	2.63	0.0036	14.16	22.35	6.02	7.62	Skin	27	0.356	$[(\pm45/\pm45)_2/90/\pm45\pm45/\overline{90}]_s$	Discrete stiffener / No 0° plies in skin
									Stiffener	78	1.030	$[90_2/\pm45/0_6/\pm45/0_7/\pm45/0_7/\pm45]_s$	
									Flange	67	0.884	$[90_2/\pm45/\pm45/0_{13}/\pm45/0_{13}/\pm45/0_{12}/\pm45/90_2]_T$	
4	Bolted	A	2.63	0.0029	18.21	15.24	6.02	7.21	Skin	27	0.356	$[(\pm45/\pm45)_2/90/\pm45/0_7/\pm\overline{90}]_s$	Discrete stiffener / No 0° plies in skin / Bolted
									Stiffener	78	1.050	$[90_2/\pm45/0_6/\pm45/0_7/\pm45/0_7/\pm\overline{45}]_s$	
									Flange	67	0.871	$[90_2/\pm45/\pm45/0_{13}/\pm45/0_{13}/\pm45/0_{12}/\pm45/90_2]_T$	
5	Bonded	B	2.63	0.0044	14.16	22.35	6.02	7.62	Skin	22	0.356	$[(\pm45/\pm45)_2/90/\pm45]_s$	Discrete Stiffener / No 0° plies in skin / Tough resin
									Stiffener	70	1.030	$[90_2/\pm45/0_5/\pm45/0_6/\pm45/0_6/\pm45]_s$	
									Flange	60	0.884	$[90_2/\pm45/0_{11}/\pm45/0_{11}/\pm45/0_{11}/\pm45/90_2]_T$	
6	Bonded	A	3.33	0.0048	18.31	15.24	5.44	7.62	Skin	38	0.503	$[(\pm45/\pm45)_2/\pm45/90_4/\pm45/90_2/\pm\overline{45}]_s$	Discrete stiffener
									Stiffener	101	1.330	$[\pm45/\pm45/0_7/\pm45/90/0_7/\pm45/90/0_7/\pm45/0_7/\pm45/\overline{90}]_s$	
									Flange	23	0.305	$[(\pm45/\pm45)_2/90/\pm45/\overline{90}]_s$	
7	Bonded	B	2.63	0.0051	17.58	15.24	5.44	7.62	Skin	28	0.554	$[(\pm45/\pm45)_2/90_3/\pm45/\overline{0_2}]_s$	Discrete stiffener / Tough resin
									Stiffener	69	1.270	$[\pm45/\pm45/0_7/\pm45/0_3/90/0_3/\pm45/0_7/\pm45/\overline{90_2}]_s$	
									Flange	18	0.254	$[(\pm45/\pm45)_2/\overline{90_2}]_s$	

TABLE IV.- INITIAL CONDITIONS AND RESULTS OF IMPACT TESTS ON BLADE-STIFFENED PANELS

Panel			Initial loading		Conditions at impact				Residual strength		Comments
Number	Width, cm	Length, cm	N_x, MN/m	ε_x	N_x, MN/m	$\varepsilon_{x_{skin}}$	Velocity, m/sec	Impact location	N_x, MN/m	ε_x	
1A	36.60	48.08	3.92	.0053	– 2.63 –	– .0035 –	– 99.97 –		2.78	.0037	Carried load without failure. Local damage without propagation. Damage caused by impact propagated in skin to lateral free edges of panel. Load reduced to 2.07 MN/m. Stiffeners undamaged and still attached to skin ±45 plies.
1B	34.29	51.59 50.80	3.89	.0052	– 3.12 –	– .0041 –	– 97.23 –				Carried load without failure. Damage initiated by impact propagated in skin 0° interface plies to lateral edges of panel. Load reduced to 2.59 MN/m. Stiffeners undamaged and still attached to skin ±45 plies. Test terminated.
2	35.56	20.00	3.75	.0052	– 2.99 2.99 –	– .0045 .0045 –	– 59.44 98.15 –		2.98	.0045	Carried load without failure. Load held. No visible damage. Damage initiated by impact propagated in skin 0° interface plies to lateral edges of panel. Load reduced to 2.49 MN/m. Stiffeners undamaged and still attached to skin ±45 plies. Failure of stiffeners.
3	59.54	50.55	2.64	.0034	– 2.61 –	– .0038 –	– 90.22 –		> 3.77	>.0050	Carried load without failure. Skin buckling at maximum load. Load held. Impact caused local damage in skin which did not propagate. At 3.29 MN/m damage propagated in skin to adjacent stiffeners and stopped. Panel loaded to 3.77 MN/m without further damage propagation. Fully developed skin buckle at maximum load. Test terminated without failure.
4	48.26	48.36	4.43	.0053	– 3.70 3.73 –	– .0046 .0044 –	– 93.88 94.79 –		4.69	.0056	Carried load without failure. Load held. Impact caused local damage which did not propagate. Load held. Local depression on impact side, no visible damage on back side. Failure by propagation of damage across panel at midlength. Stiffeners also failed. Bolt heads pulled through skin laminate.
5	59.54	50.52	2.61	.0040	– 2.64 –	– .0045 –	– 90.22 –		3.43	.0054	Carried load without failure. Skin buckle well developed. Load held. Impact caused local damage in skin which did not propagate. Failure by brooming in end region. No evidence of damage growth in impact region.
6	45.80	50.57	3.15	.0046	– 2.75 –	– .0050 –	– 93.57 –		3.08	.0045	Carried load without failure. Load held. Impact caused local damage in skin which extended up to but not into stiffener region. Delamination damage initiated by impact propagated in skin to lateral edges of panel. Load dropped to 2.80 MN/m primarily carried by stiffeners.
7	45.75	50.65	2.94	.0057	– 2.36 –	– .0054 –	– 85.95 –		2.85	.0060	Carried load without failure. Load held, impact caused local damage in skin which did not propagate. Failure by disbond of stiffeners from skin. Inspection indicated poor bond. No evidence of damage growth in impact region.

(c) Mechanically fastened plate.

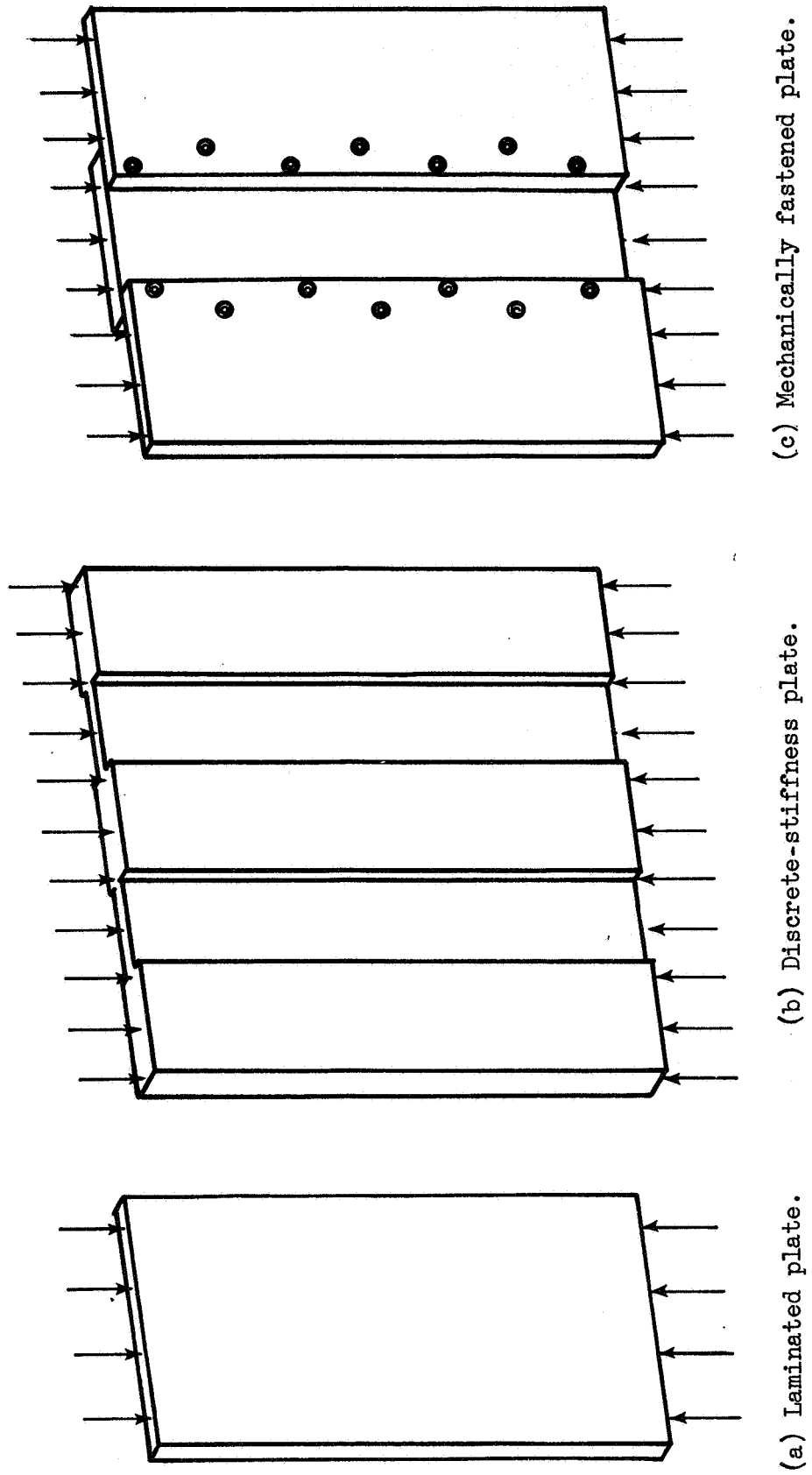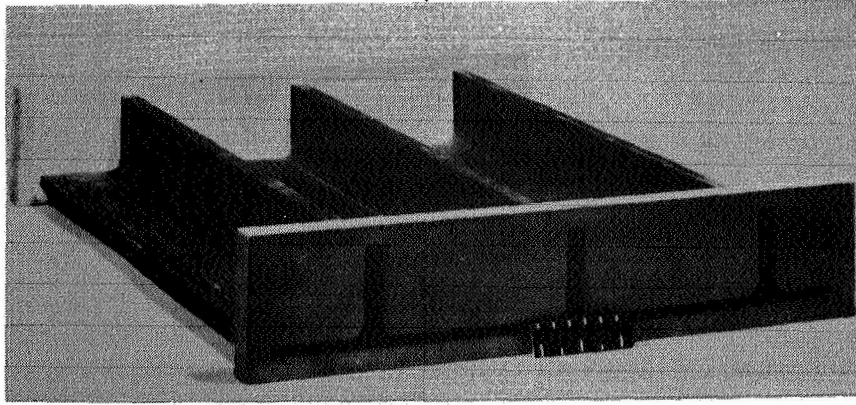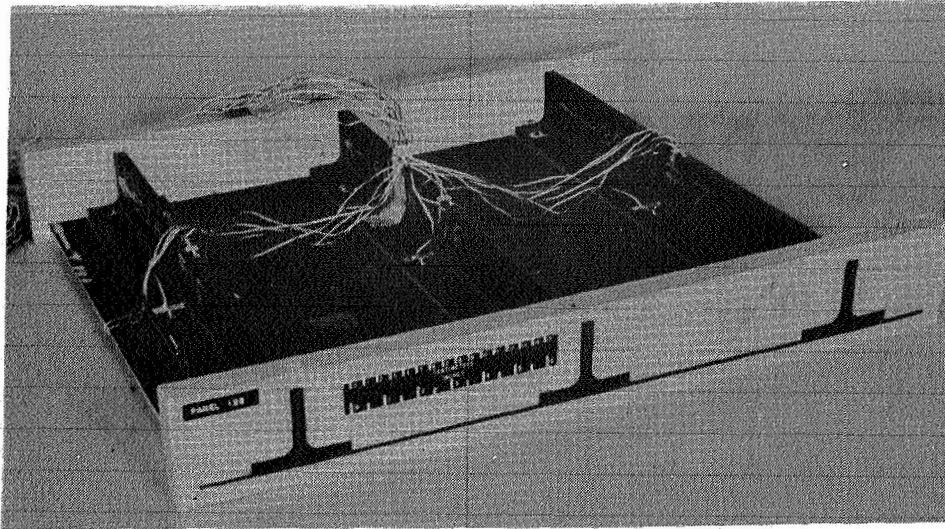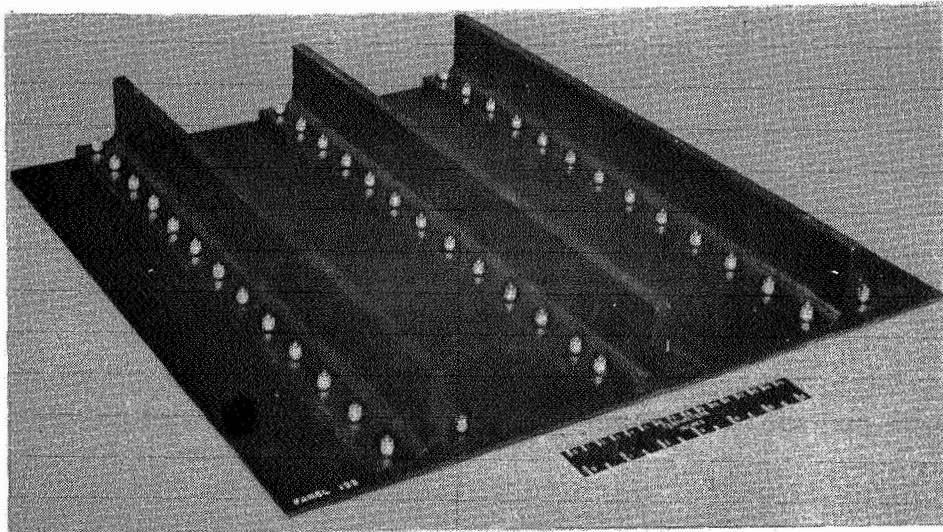(b) Discrete-stiffness plate.

(a) Laminated plate.

Figure 1.- Flat plate test specimens.

(a) Panel with cocured stiffeners.

(b) Panel with bonded stiffeners.

(c) Panel with bolted stiffeners.
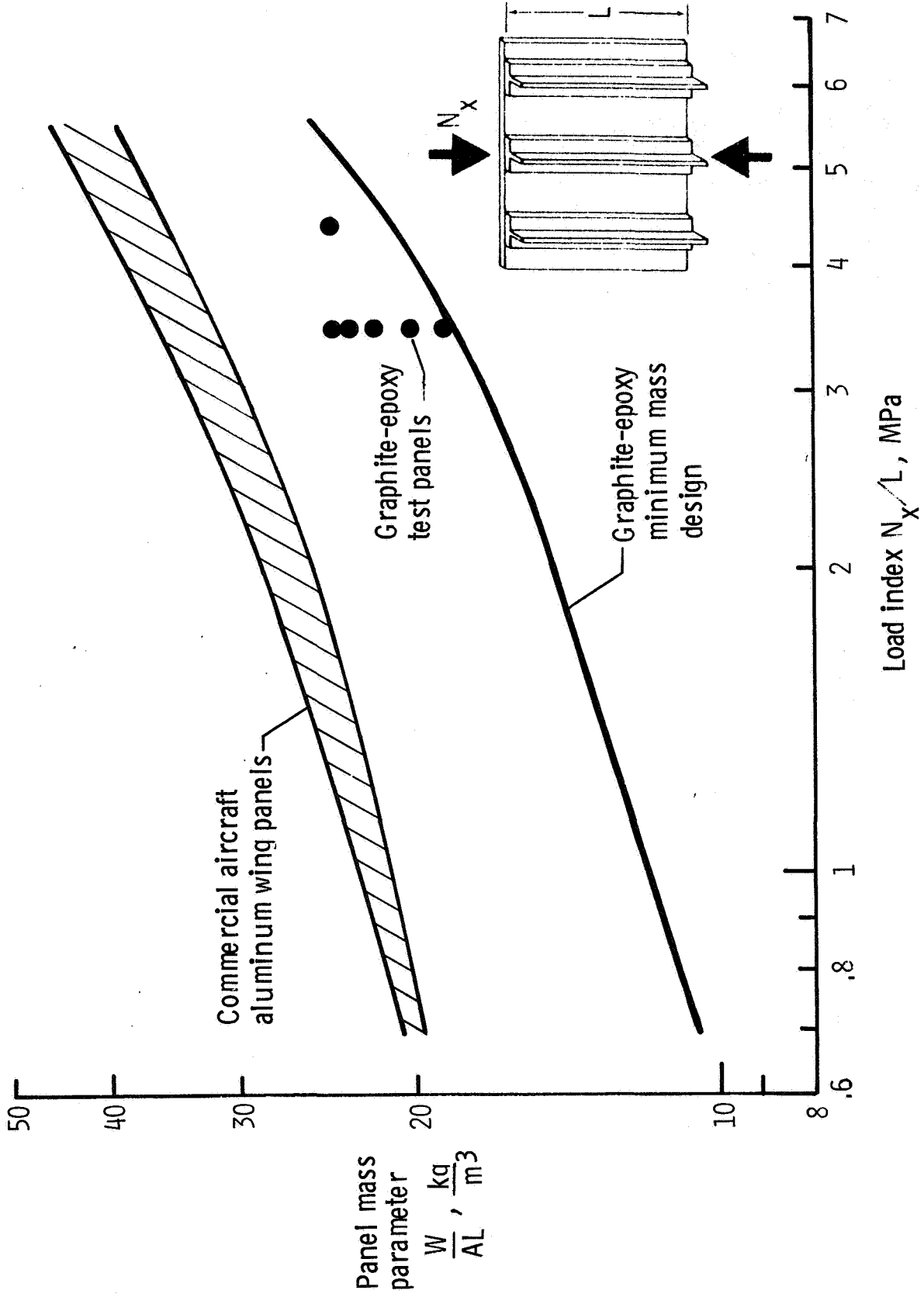
Figure 2.- Blade-stiffened test panels.

Figure 3.- Comparison of structural efficiency of blade-stiffened compression test panels with minimum mass designs.
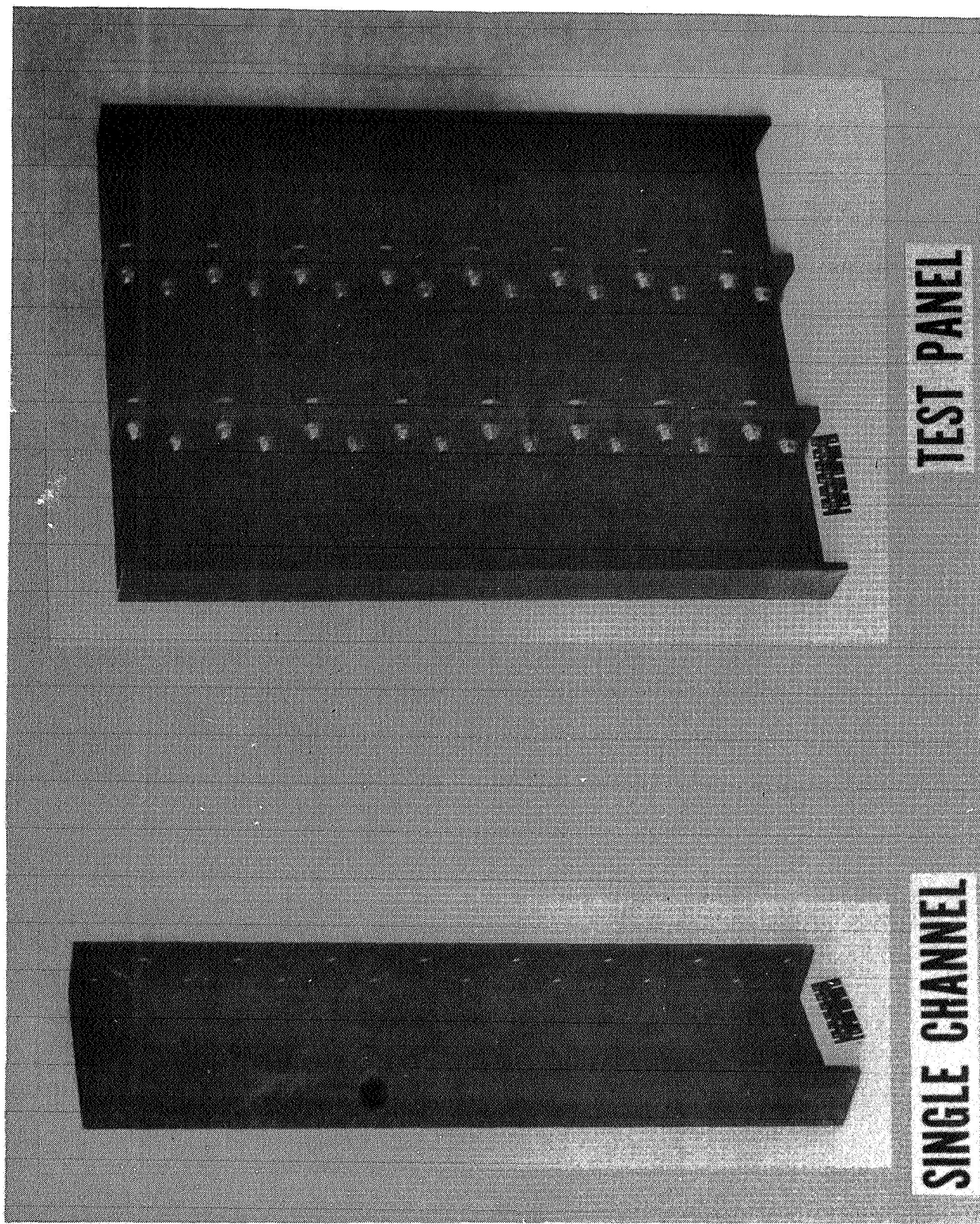
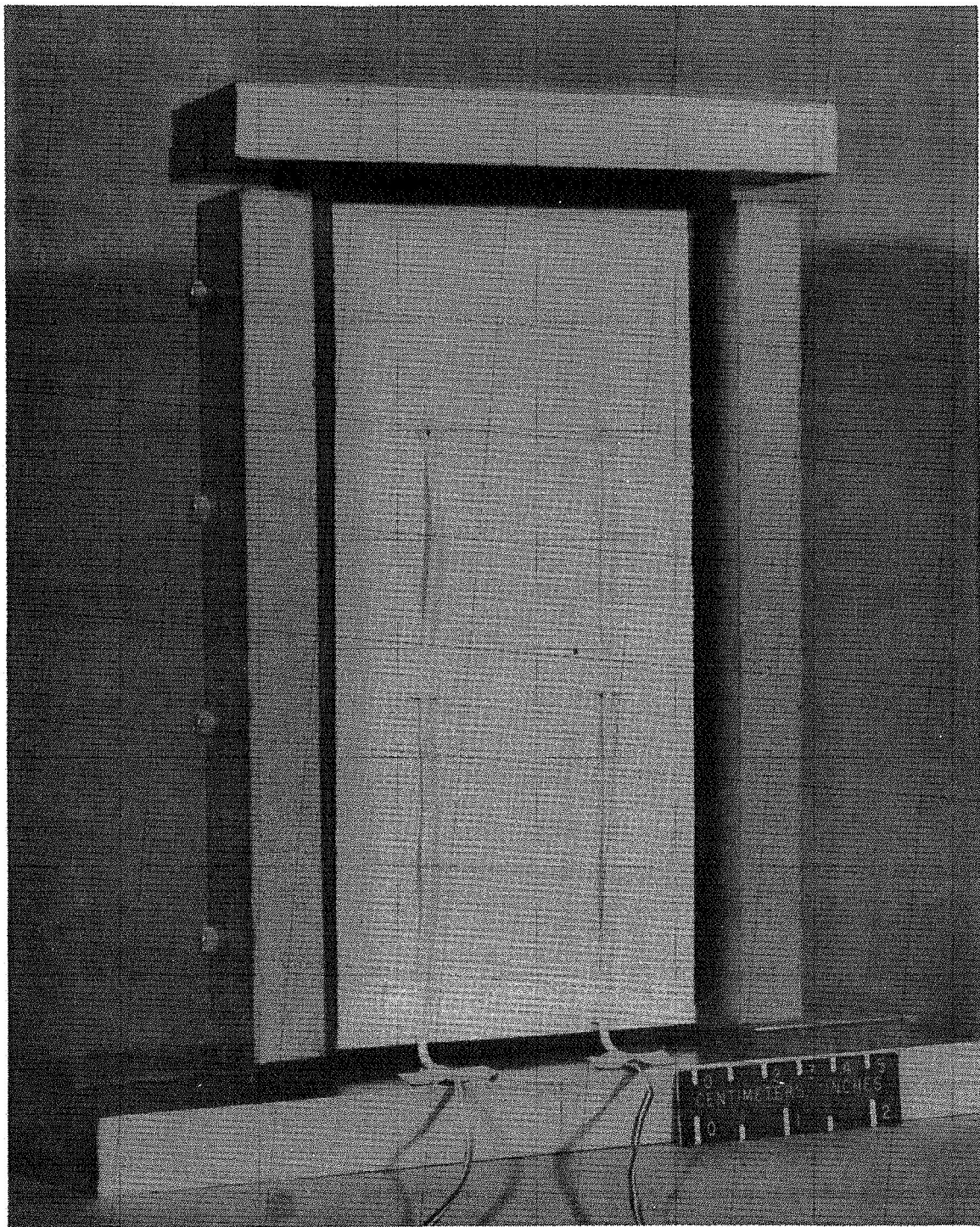Figure 4.- Mechanically fastened blade-stiffened panel fabricated from single channel sections.

Figure 5.- Laminated plate specimen mounted in supporting test frame.

● Failed on impact
○ Did not fail on impact
■ Residual strength

(a) Material A (specimen group P1).

(b) Material B (specimen group P2).

(c) Material C (specimen group P3).

(d) Failure-threshold curves for Materials A, B, and C.
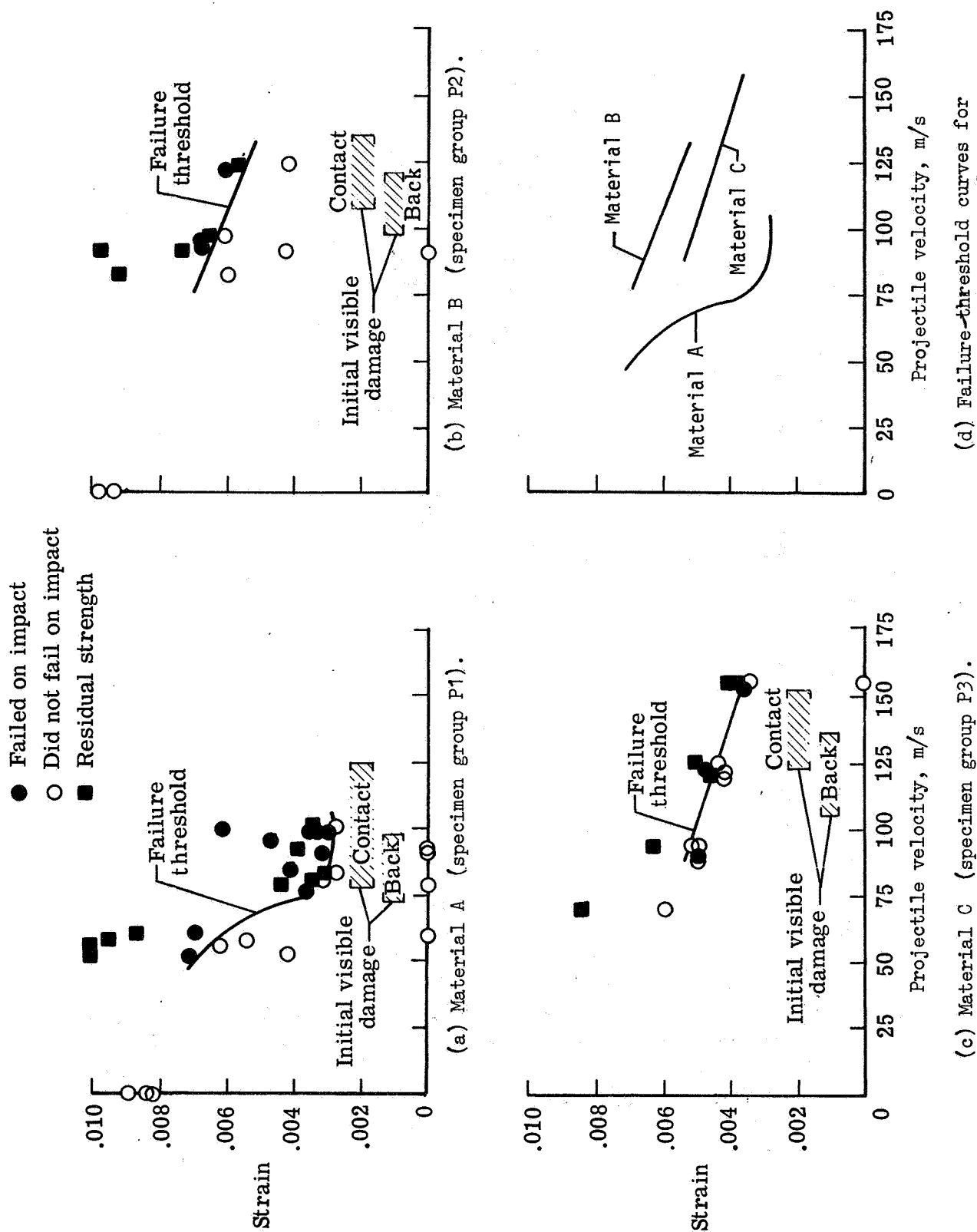
Figure 6.- Comparison of impact damage on the compression strength of laminated plate specimens with different materials.
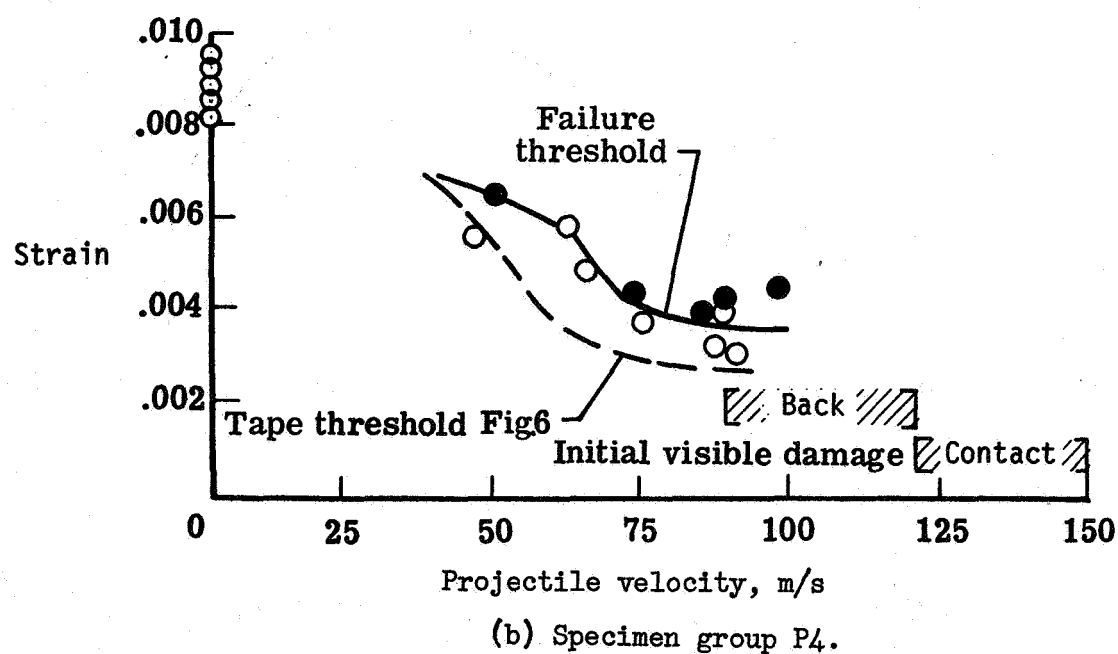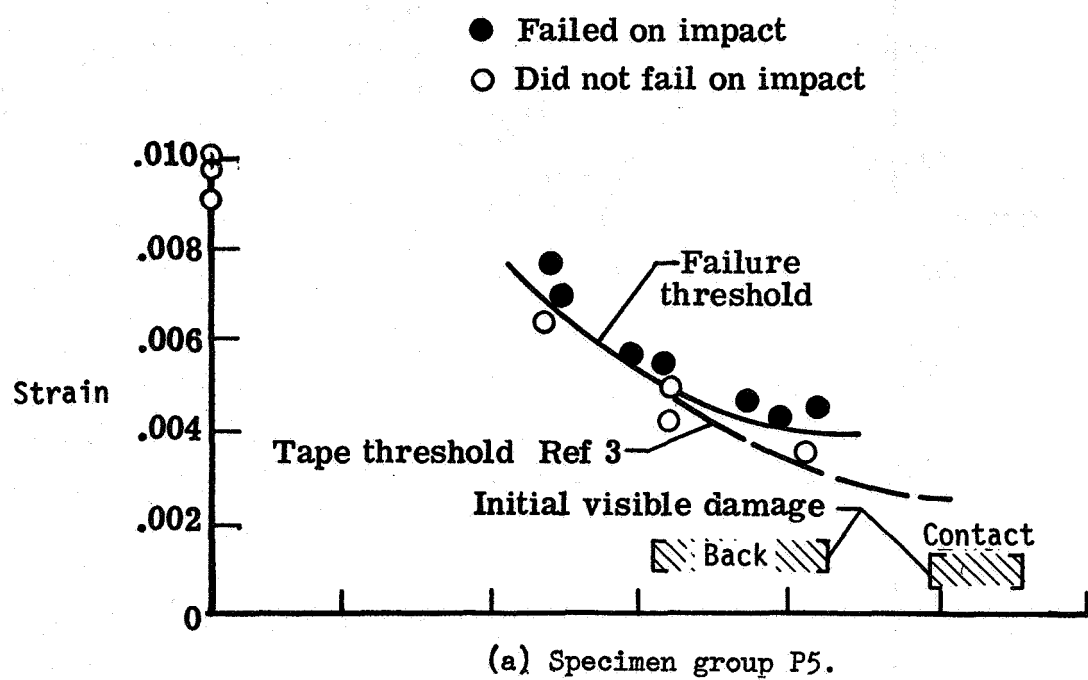
Figure 7.- Effect of impact damage on graphite fabric Material A.

(a) Material A (specimen group RP1).

(b) Material B (specimen group RP2).

(c) Material A with tape and fabric (specimen group RP3).
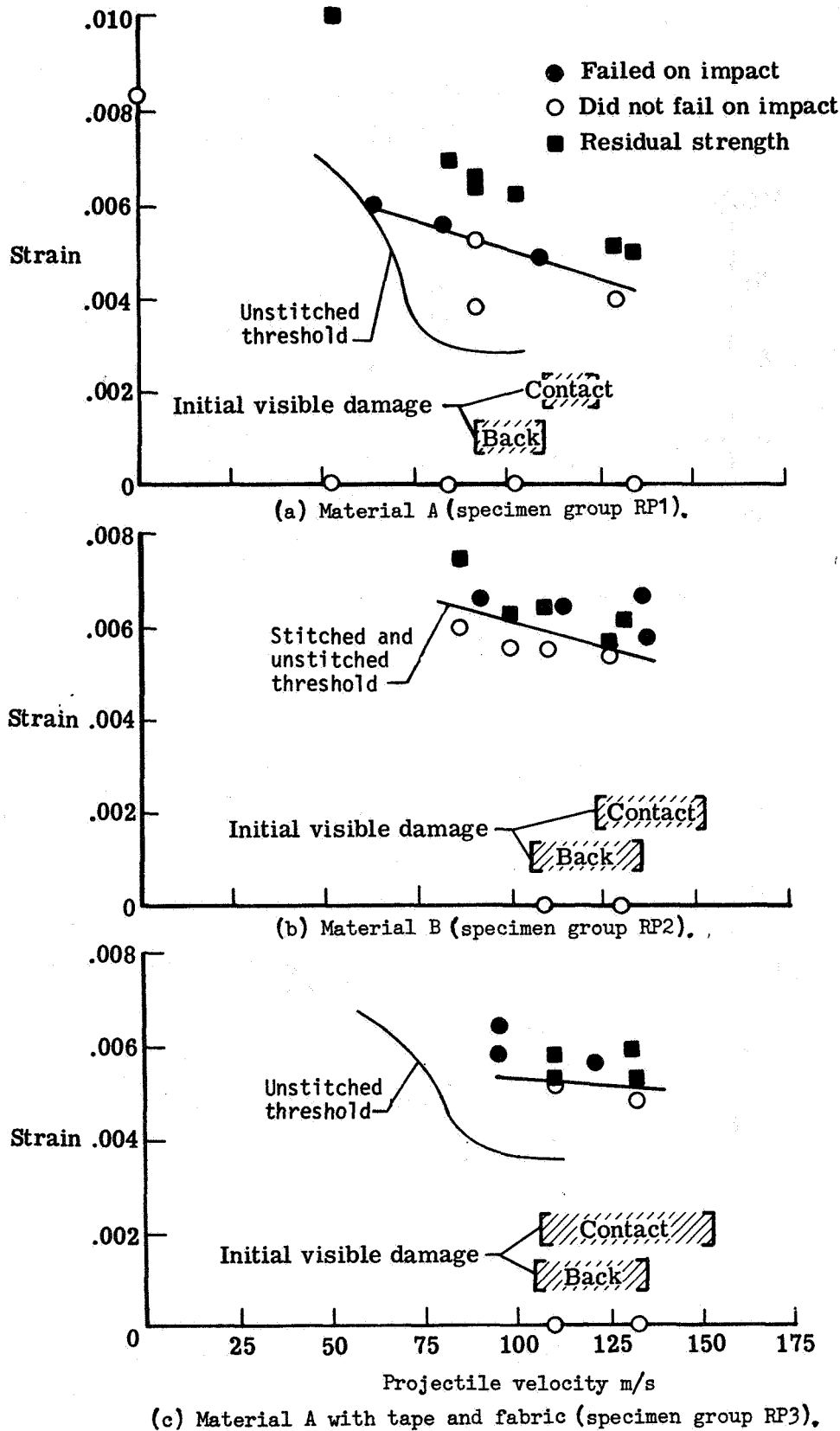
Figure 8.- The effect of transverse reinforcement on the compression strength of laminated plate specimens with impact damage.
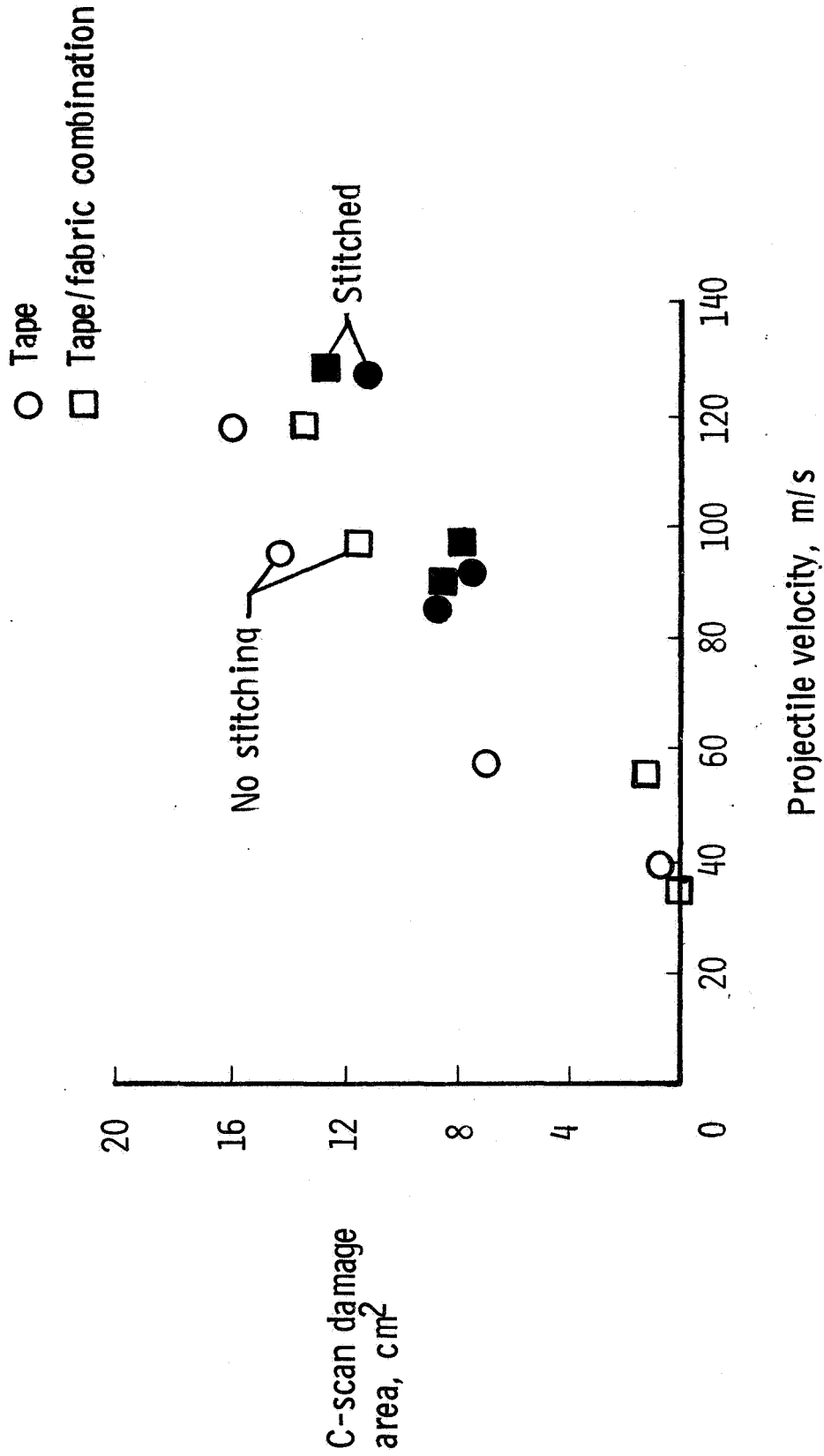
Figure 9.- Damaged area in Material A laminates with and without transverse reinforcement.
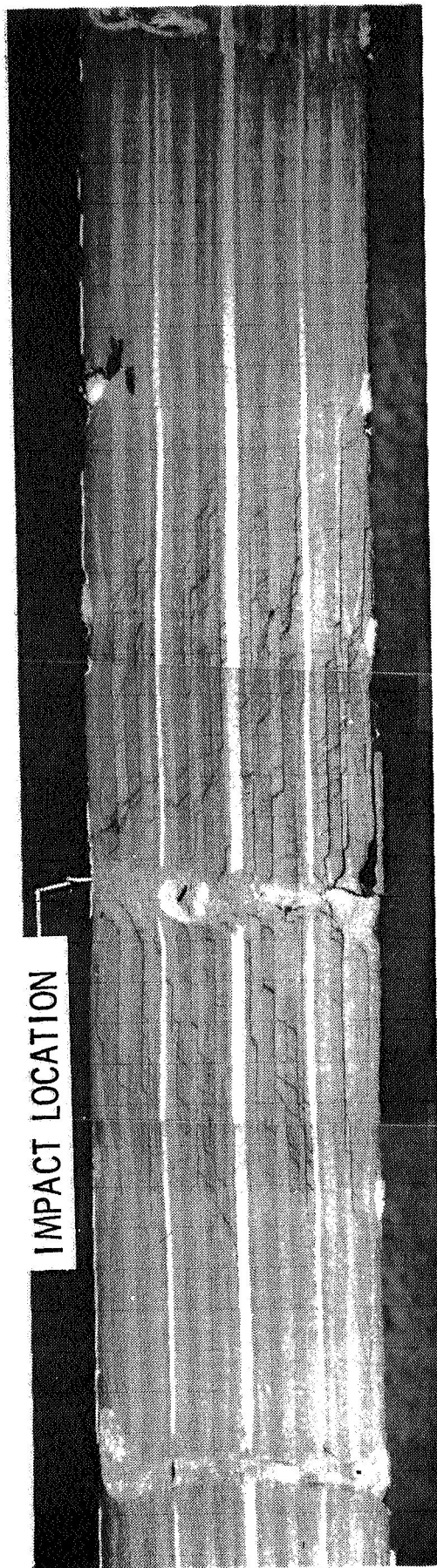
(a) Impact velocity 86 m/s.
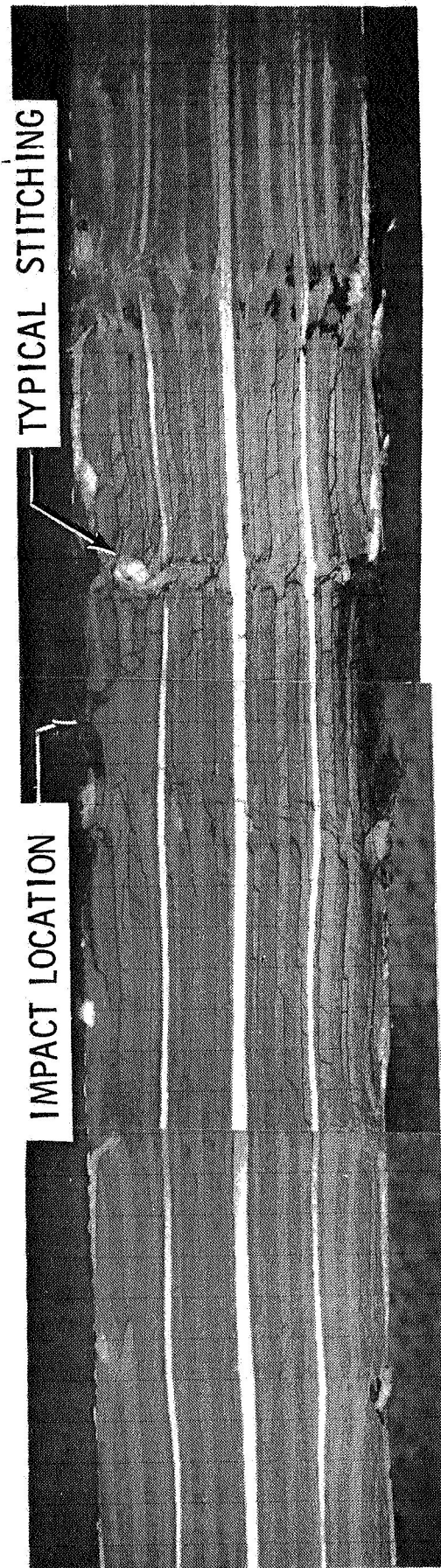
(b) Impact velocity 128 m/s.

Figure 10.- Cross-section of test laminate of Material A (specimen group RP1) with transverse reinforcement after damage by impact.
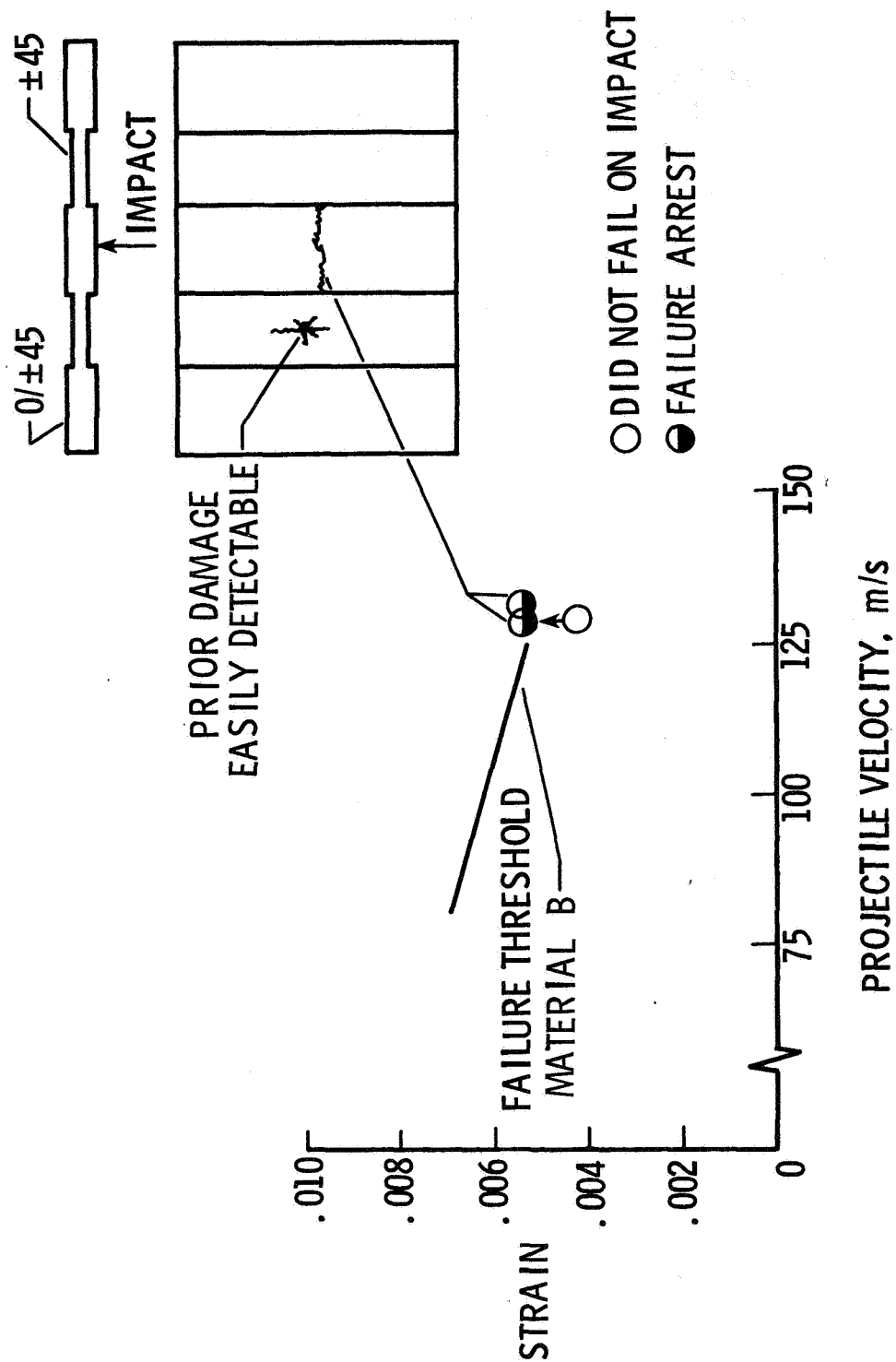
Figure 11.- Effect of impact on discrete-stiffness flat panels.
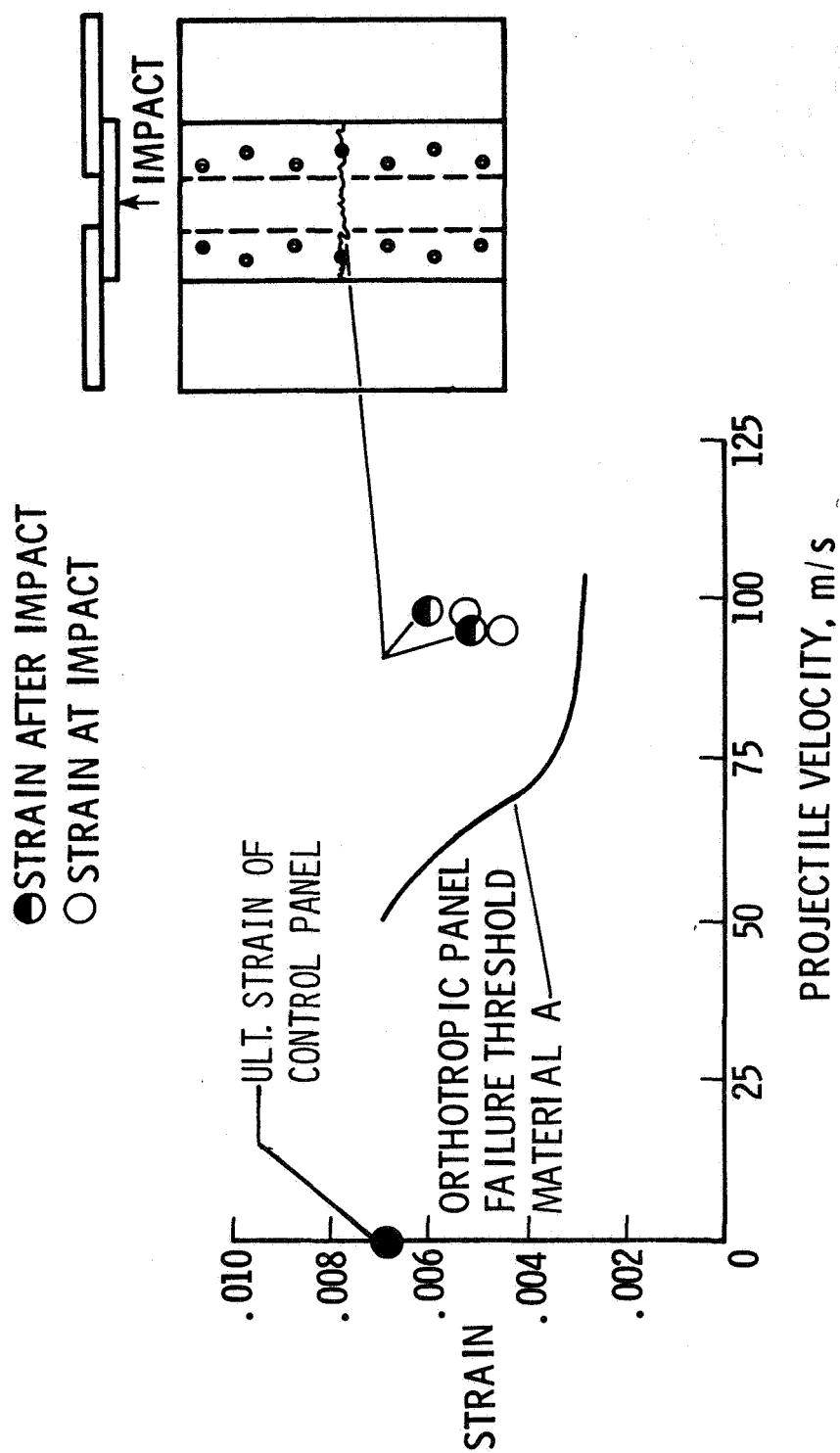
Figure 12.- Effect of impact on mechanically fastened flat panels.
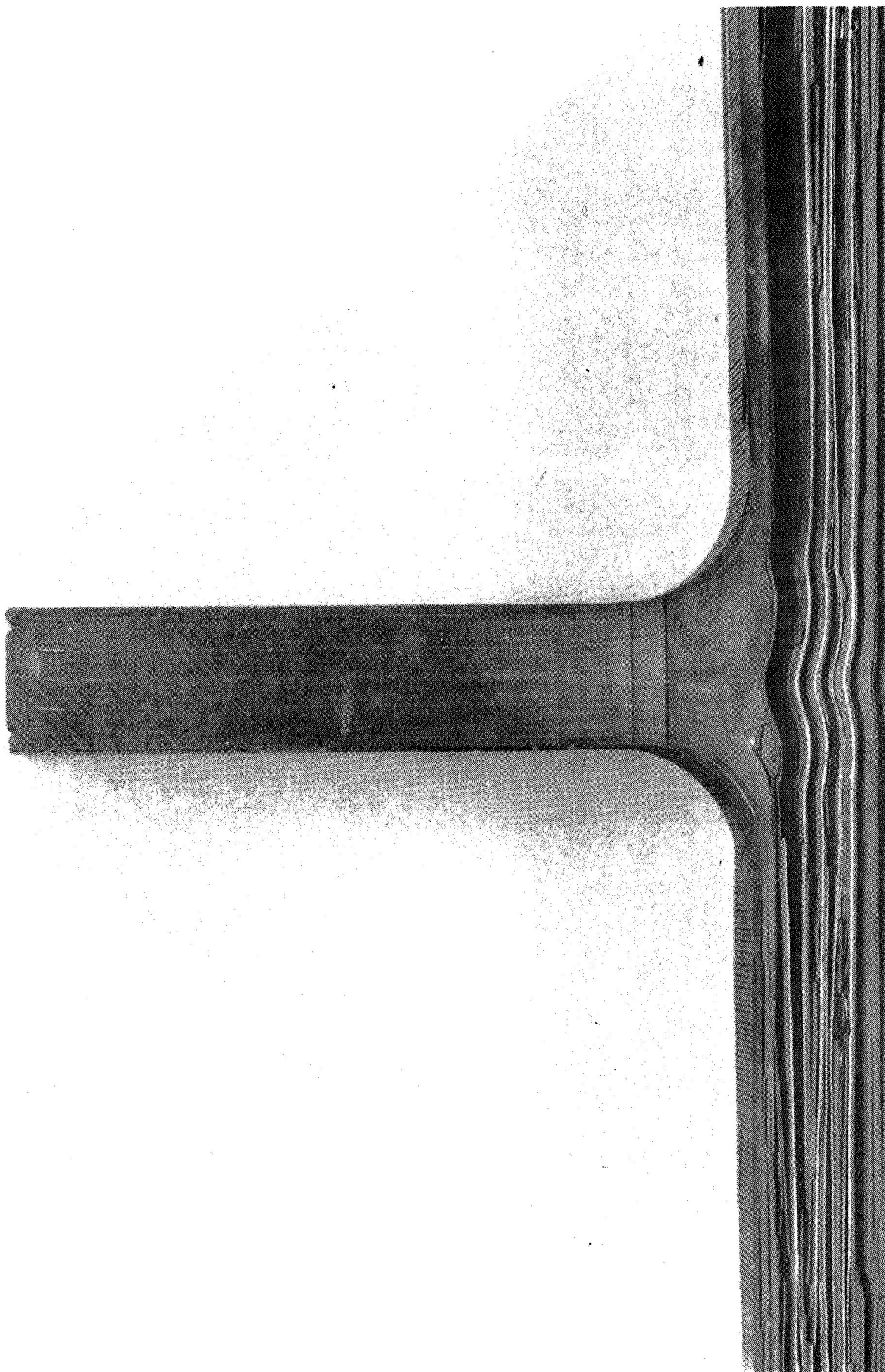
Figure 13.- Skin delamination in cross-section of cocured panel after impact test.
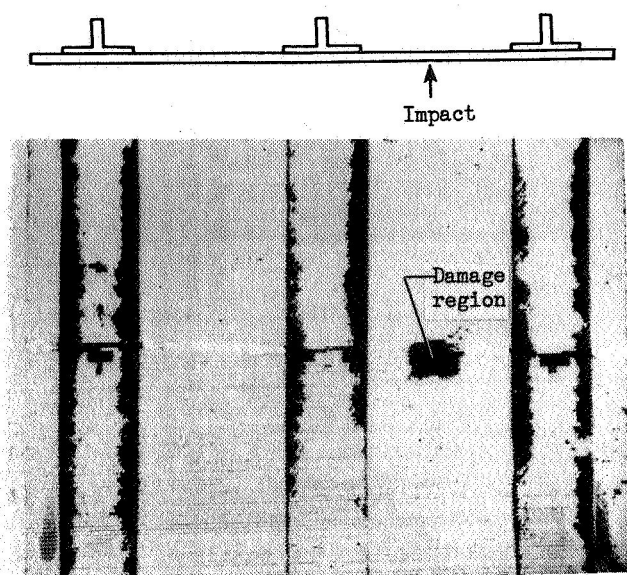
(a) C-scan of initial damage in panel.

(b) C-scan after damage propagation.

(c) Load/strain response during test.
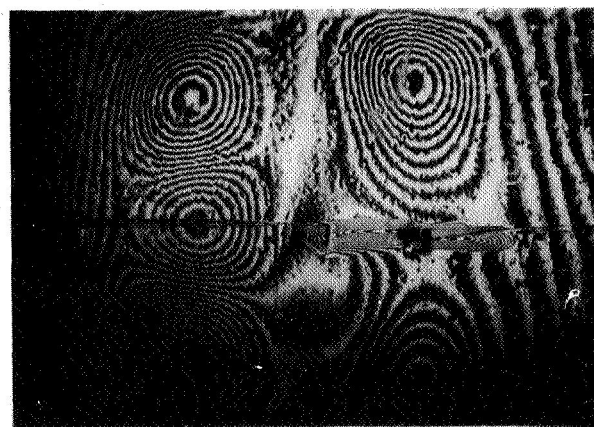
(d) Moire-fringe photo after damage propagation.

Figure 14.- Test results for panel 3 showing skin delamination arrest at stiffeners.
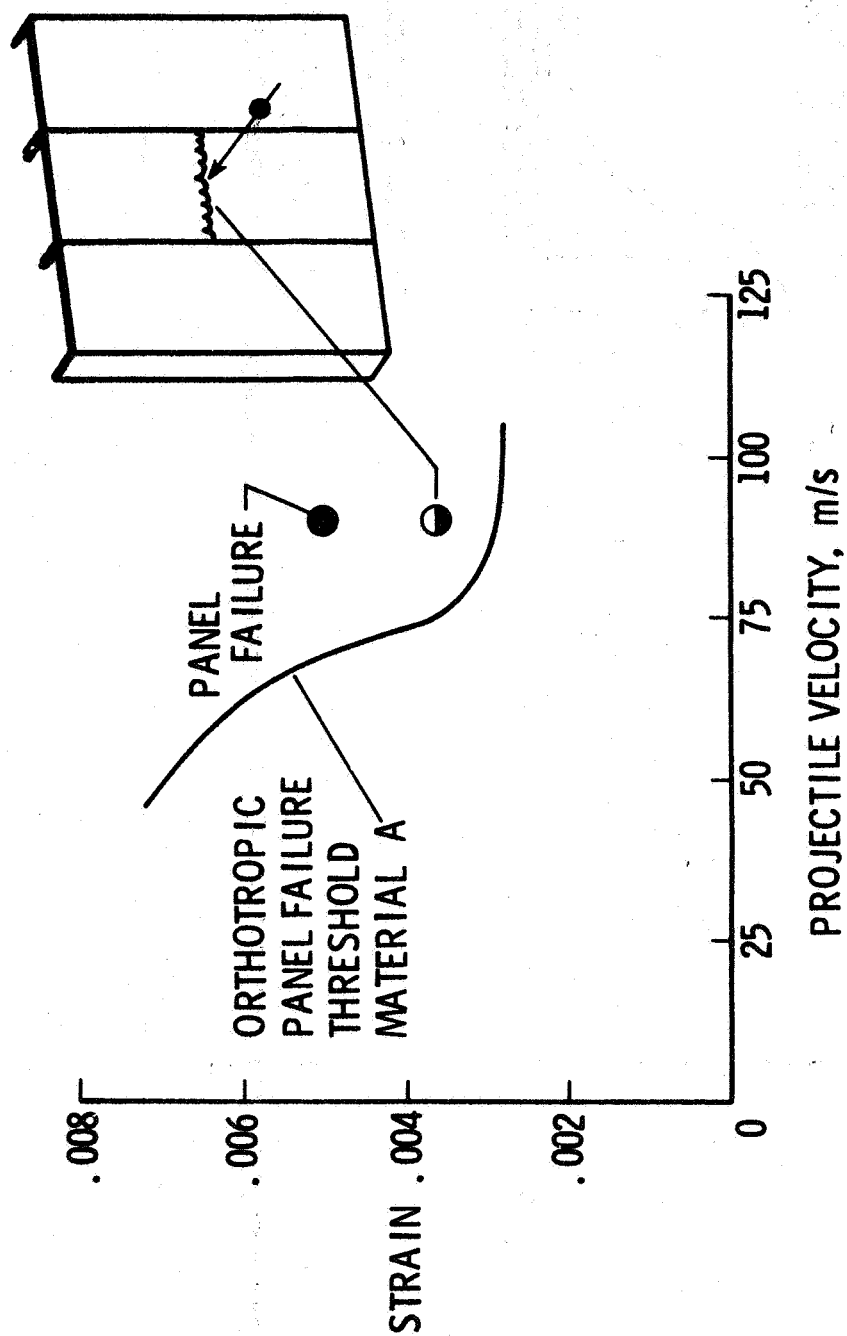
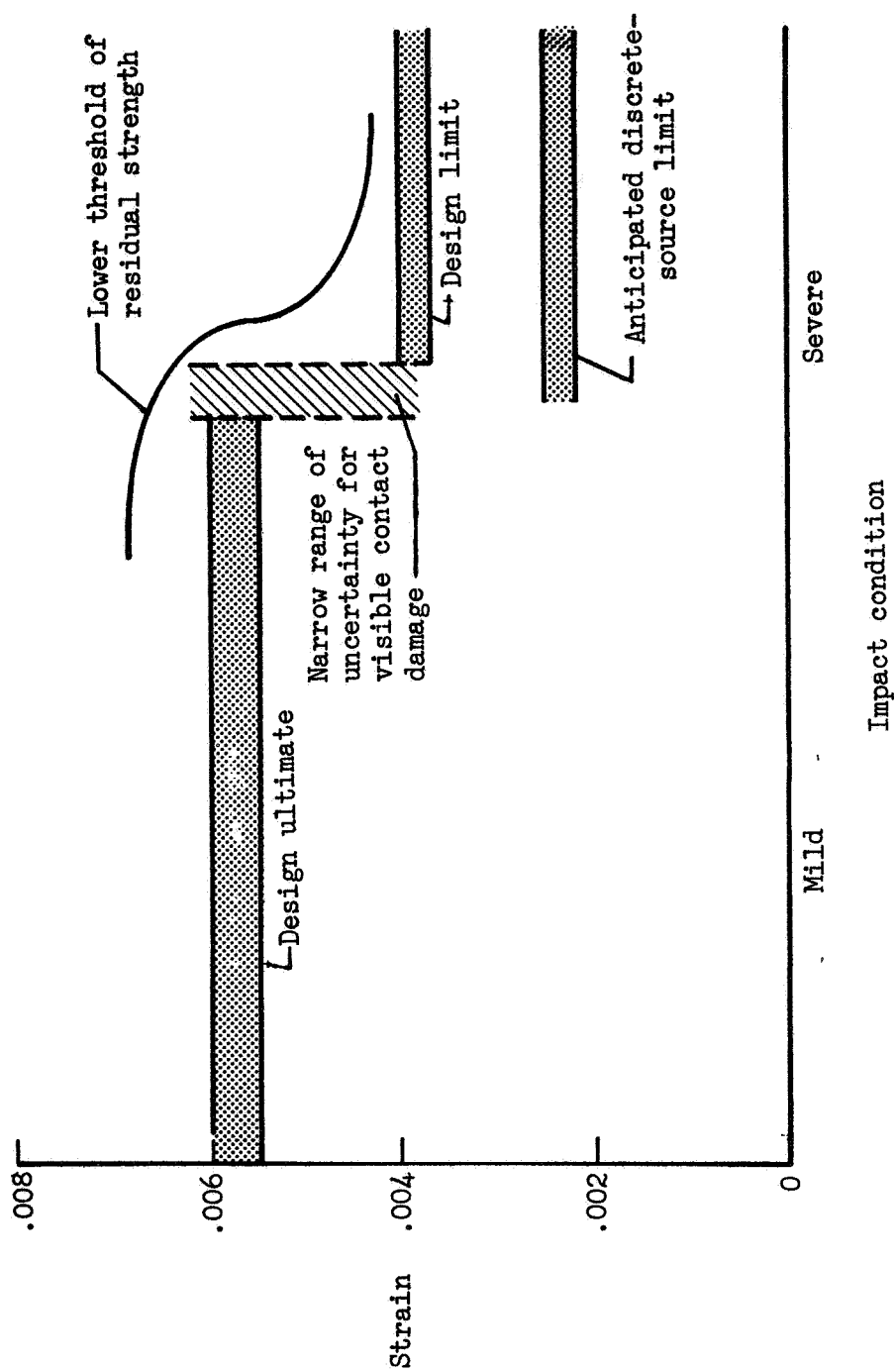Figure 15.– Impact initiated failure on blade-stiffened panels fabricated from channel sections.

Figure 16.- Desirable impact properties of composite materials based on
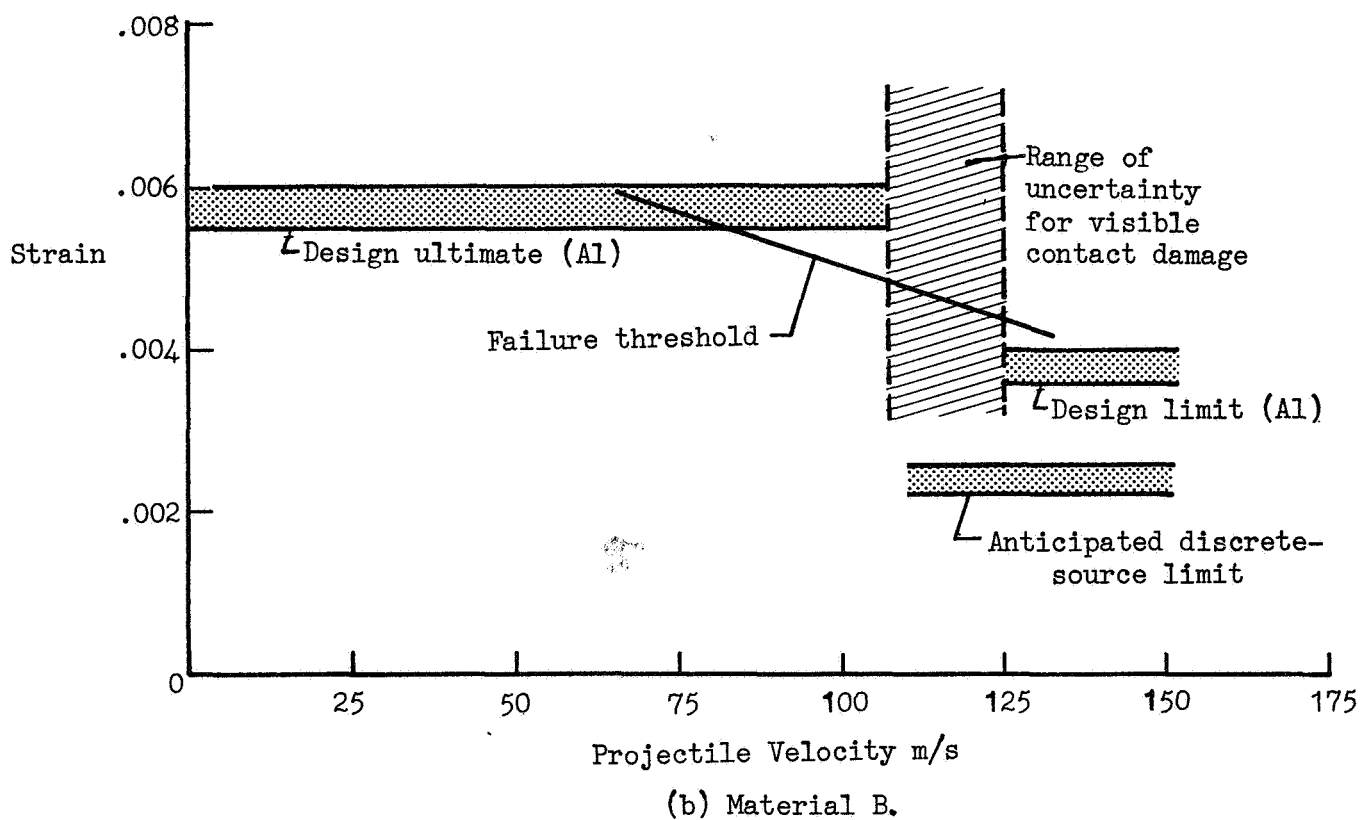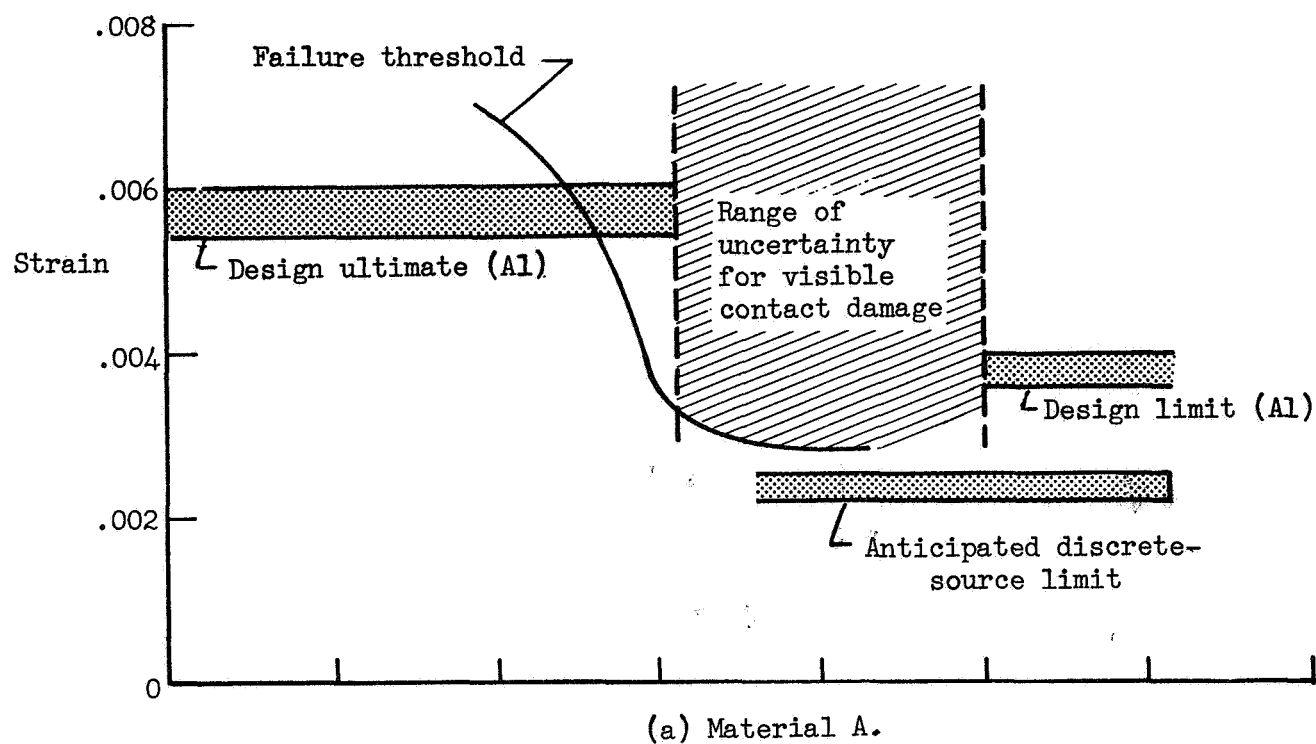current aircraft design considerations.

(a) Material A.

(b) Material B.

Figure 17.- Comparison of test materials with current aircraft design considerations.
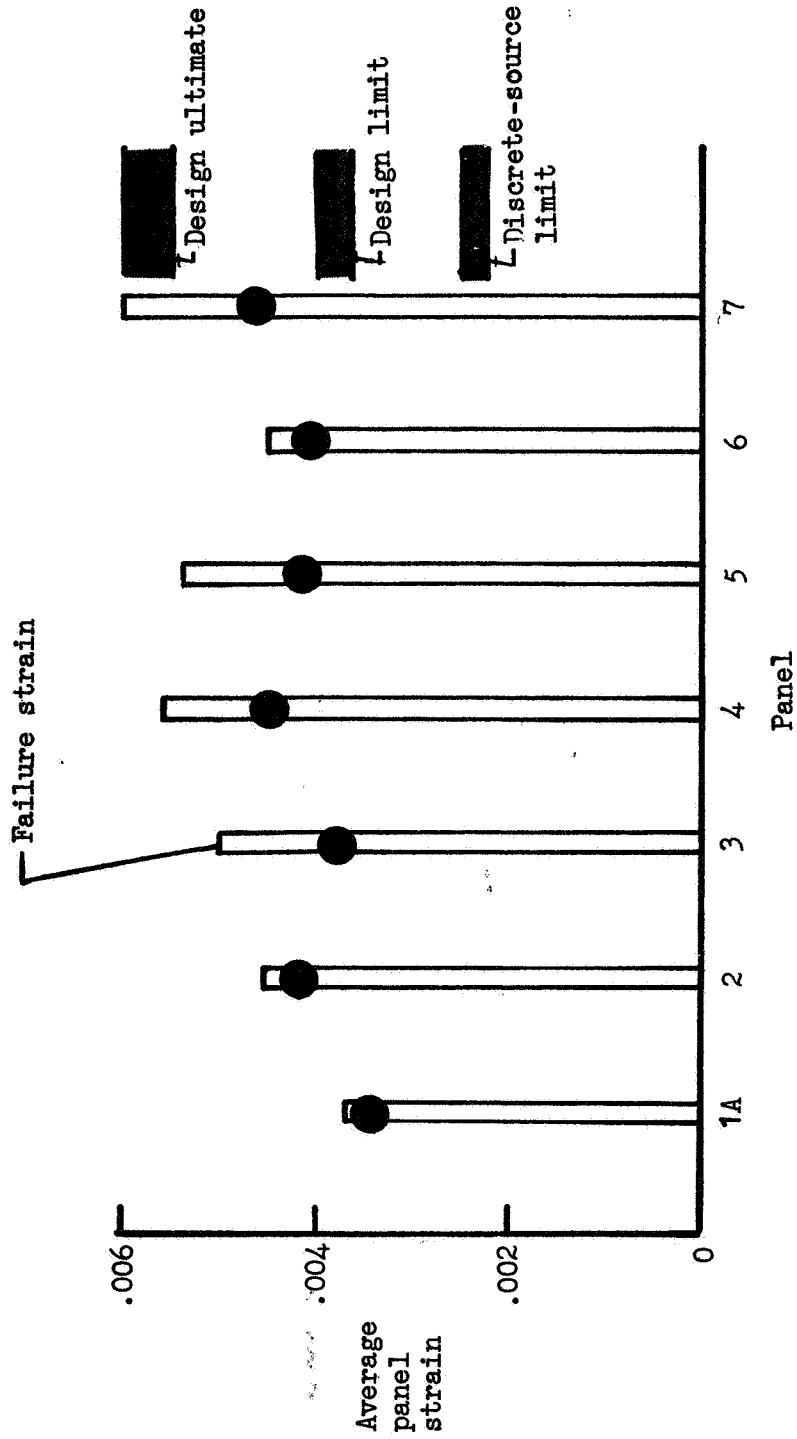
Figure 18.- Comparison of blade-stiffened test panels with current aircraft design considerations.
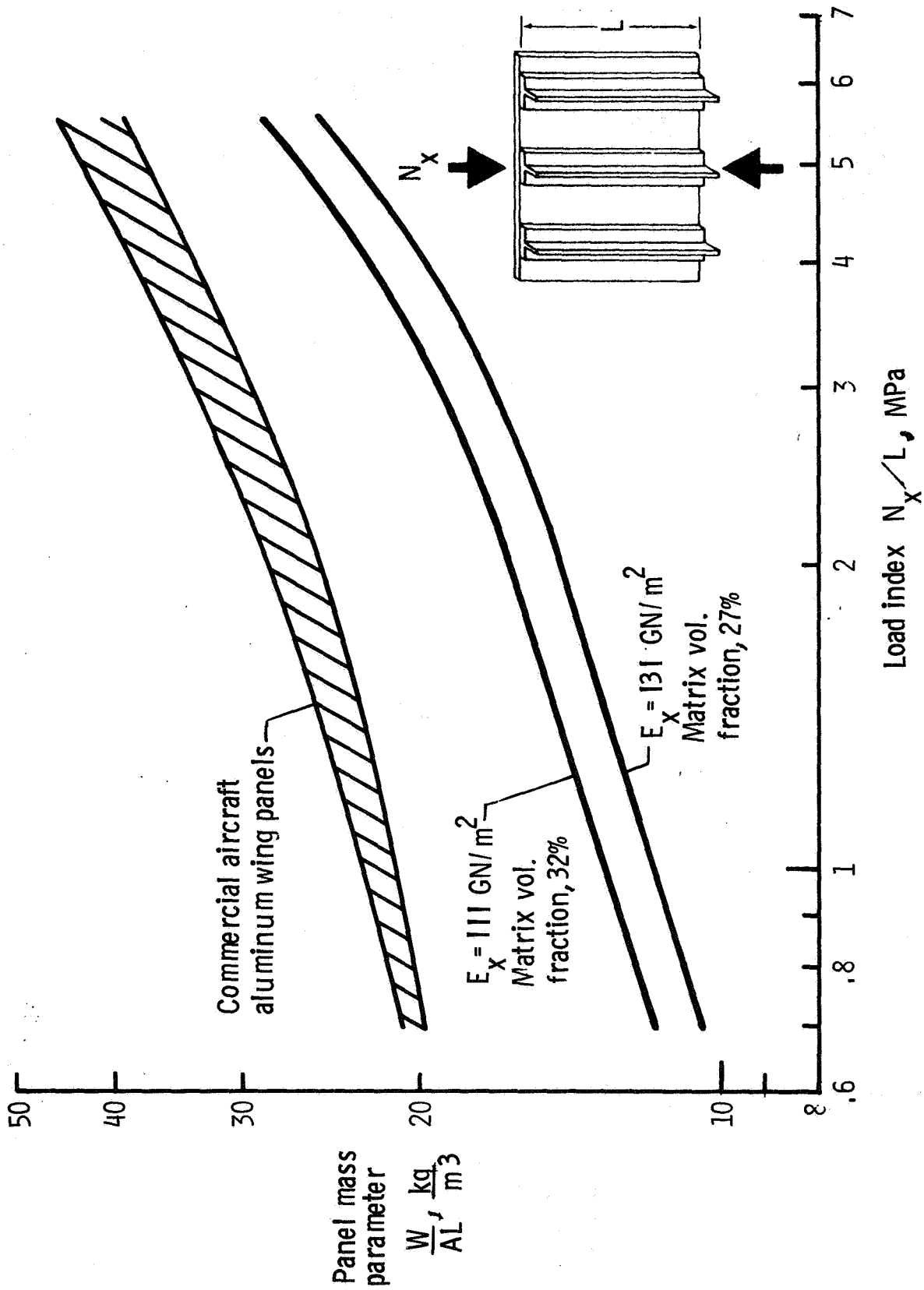
Figure 19.- Effect of material modulus on the structural efficiency of graphite-epoxy blade-stiffened panels.
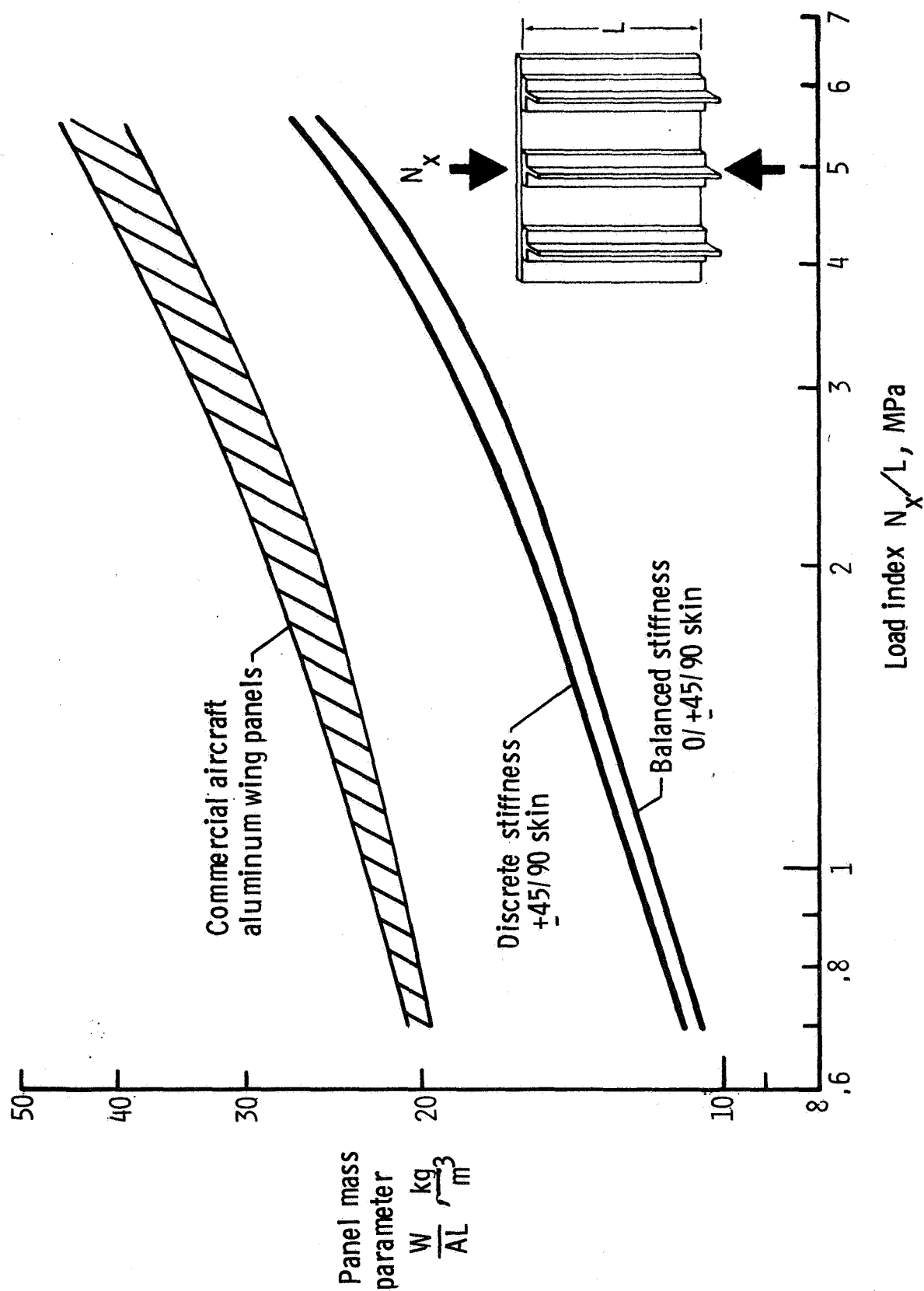
Figure 20.- Effect of discrete-stiffness design on the structural efficiency of graphite-epoxy blade-stiffened panels.

1. Report No. NASA TM-85748	2. Government Accession No.	3. Recipient's Catalog No.
4. Title and Subtitle Concepts for Improving the Damage Tolerance of Composite Compression Panels		5. Report Date February 1984
		6. Performing Organization Code 534-06-23
7. Author(s) Marvin D. Rhodes Jerry G. Williams		8. Performing Organization Report No.
9. Performing Organization Name and Address NASA-Langley Research Center Hampton, VA 23665		10. Work Unit No.
		11. Contract or Grant No.
12. Sponsoring Agency Name and Address National Aeronautics and Space Administration Washington, DC 20546		13. Type of Report and Period Covered Technical Memorandum
		14. Sponsoring Agency Code

15. Supplementary Notes

Paper presented at Fifth Conference on Fibrous Composites in Structural Design. New Orleans, Louisiana, January 1981

16. Abstract

An experimental investigation was conducted to evaluate concepts both for improving the strength of graphite-epoxy compression panels when subjected to impact damage, and for arresting damage propagation. The tests were conducted on flat plate specimens and blade-stiffened structural panels which have application in heavily-loaded commercial aircraft wings. The residual strength of specimens with damage and the sensitivity to damage while subjected to an applied inplane compression load were determined. The results suggest that matrix materials that fail by delamination have the lowest damage tolerance capability. Alternate matrix materials or laminates which are transversely reinforced suppress the delamination mode of failure and change the failure mode to transverse shear crippling which occurs at a higher strain value. Several damage-tolerant blade-stiffened panel design concepts were evaluated. Not permitting 0° plies to traverse into the stiffener proved successful in suppressing stiffener failure by delamination. Bonding stiffeners to the skin was successful in arresting damage propagation for designs in which the stiffener and stiffener flange were sufficiently stiff (thick) to restrict the transverse deformations of the propagating skin delamination. A bolted-stiffener design has the potential for redistributing load from a failed region but needs further evaluation using longer panels. Structural efficiency studies conducted show only small mass penalties may result from incorporating these damage-tolerant features in panel design. Finally, the implication of test results on the design of aircraft structures was examined with respect to FAR requirements.

17. Key Words (Suggested by Author(s)) Composite Structures Impact Damage Damage Tolerance Structural Concepts	18. Distribution Statement Unclassified - Unlimited Subject Category 39

19. Security Classif. (of this report) Unclassified	20. Security Classif. (of this page) Unclassified	21. No. of Pages 41	22. Price A03